

CMS Paper

2009/12/16

Performance of the CMS Drift-Tube Chamber Local Trigger with Cosmic Rays

The CMS Collaboration*

Abstract

The performance of the Local Trigger based on the drift-tube system of the CMS experiment has been studied using muons from cosmic ray events collected during the commissioning of the detector in 2008. The properties of the system are extensively tested and compared with the simulation. The effect of the random arrival time of the cosmic rays on the trigger performance is reported, and the results are compared with the design expectations for proton-proton collisions and with previous measurements obtained with muon beams.

arXiv:0911.4893v2 [physics.ins-det] 16 Dec 2009

*See Appendix A for the list of collaboration members

1 Introduction

The primary goal of the Compact Muon Solenoid (CMS) experiment [1] is to explore particle physics at the TeV energy scale exploiting the proton-proton collisions delivered by the Large Hadron Collider (LHC) [2]. During October-November 2008 CMS conducted a month-long data taking exercise with the goal of commissioning the experiment for extended operation [3]. The experiment recorded 270 million cosmic ray triggered events with the solenoid at its nominal axial field strength of 3.8 T. Prior to this, and during the final installation phase of the experiment, a series of week-long commissioning exercises to record cosmic ray events took place from May to September 2008, without magnetic field. Over 300 million cosmic ray triggers were accumulated during this data taking period. The drift-tube muon system of the detector continuously provided the trigger to the experiment and enabled muon track reconstruction. The drift-tube Local Trigger is the component of the trigger system that provides the information to reconstruct muon trigger candidates in the drift-tube system.

This paper describes the performance of the drift-tube Local Trigger system determined from data collected in this data taking period. Results include measurements of the system efficiency, the performance of the bunch crossing identification, the position and angular resolution of the muon-trigger candidate, and the false dimuon trigger rate. The trigger data are also compared with software emulation. Such studies test the reliability of the system and improve the understanding of the muon trigger performance in preparation for LHC operation. The trigger system design is optimized for muons produced in bunched-beam collisions. The random arrival time of the cosmic rays degrades the average performance compared to the expectations for proton-proton collisions. However, results for particles traversing the detector with the proper timing show that the system will perform as required for muons produced at the LHC.

2 The Experimental Apparatus

The central feature of the CMS apparatus is a superconducting solenoid, of 6 m internal diameter, providing a field of 3.8 T. Within the field volume are the silicon pixel and strip tracker, the crystal electromagnetic calorimeter (ECAL), and the brass/scintillator hadron calorimeter (HCAL). Muons are measured in gas-ionization detectors embedded in the steel return yoke. In addition to the barrel and endcap detectors, CMS has extensive forward calorimetry. A detailed description of the CMS experiment can be found in Ref. [1].

CMS uses a right-handed coordinate system, with the origin at the nominal collision point, the x -axis pointing to the center of the LHC, the y -axis pointing up (perpendicular to the LHC plane), and the z -axis along the anticlockwise-beam direction. The polar angle, θ , is measured from the positive z -axis and the azimuthal angle, ϕ , is measured in the x - y plane.

The CMS experiment has a two-level trigger system: the Level-1 Trigger and the High Level Trigger. The Level-1 Trigger is composed of custom hardware processors and it uses information from the calorimeters and muon detectors to select the events with a constant latency of about $3.5 \mu\text{s}$. The High Level Trigger processor farm further decreases the event rate from a maximum input rate of 100 kHz to an event recording rate of approximately 100 Hz [4, 5].

The muon detection system covers the pseudorapidity range $|\eta| < 2.4$ with detection planes based on three different technologies: drift tubes (DT), cathode strip chambers (CSC), and resistive plate chambers (RPC) [6]. The DT system is located in the barrel part of the detector, extending over the range $|\eta| < 1.3$, whereas CSCs are used in the endcaps, in the region $0.8 < |\eta| < 2.4$. The RPC system covers the region $|\eta| < 1.6$. Combining the measured

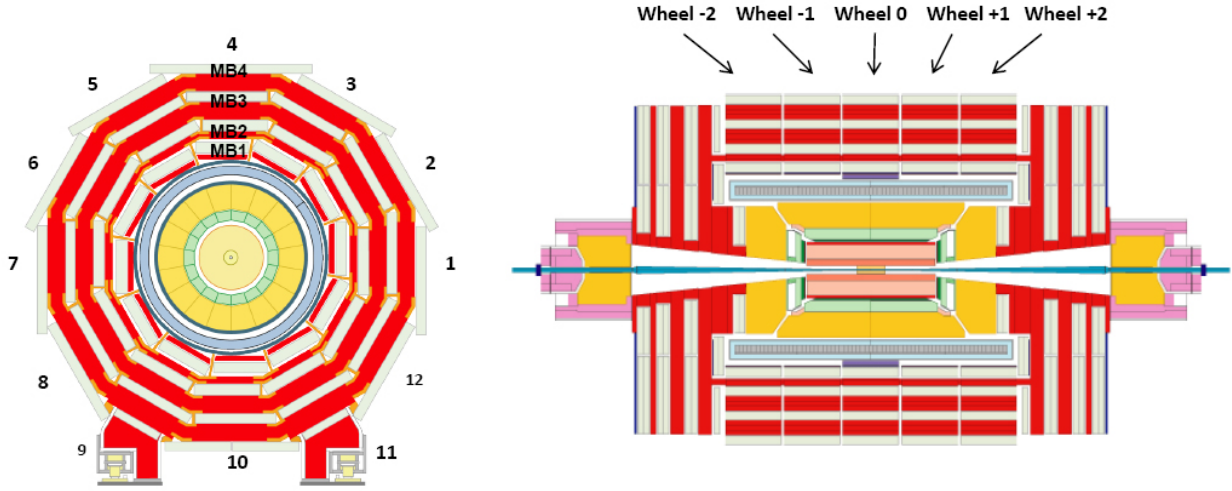


Figure 1: Left: schematic view of one of the five wheels of the muon barrel system of the CMS experiment, in the x - y plane. Right: the five wheels are visible in the longitudinal view of the CMS detector.

tracks from charged particles in the muon system with those measured in the silicon tracker results in a transverse momentum resolution between 1 and 5% for transverse momenta up to 1 TeV/ c [7]. The muon detector also provides a highly efficient muon trigger. The usage of RPCs and DTs in the barrel, and RPCs and CSCs in the endcaps, makes the system robust and redundant. Both the DT and CSC detectors perform muon tracking and participate in the Level-1 muon trigger, independently of the RPCs.

2.1 The Drift-Tube Muon System

The DT system consists of 240 muon chambers. Figure 1 shows how the muon chambers are arranged in 12 sectors with four station types in each of the five wheels of the CMS barrel. The four station types are called MB1, MB2, MB3, and MB4 from inside to outside, where MB stands for Muon Barrel. Although the chambers of station type MB4 in sectors 4 and 10 are physically divided in two parts, in this paper they are considered as a single unit. In each chamber eight layers of DT cells with wires parallel to the beam direction are arranged in two "superlayers" of four layers each, devoted to trigger and position measurements in the x - y plane. With the exception of type MB4, all chambers are equipped with an extra "superlayer" of four layers to perform measurements along the z coordinate using DT cells with wires orthogonal to the beam direction.

Chambers are equipped with Time to Digital Converter (TDC) units, which measure the drift time in each cell, as well as with dedicated electronics to perform the Level-1 trigger algorithm. For tracking purposes, the signals recorded by the TDC units are converted to position coordinates (called "hits") using the space-time relation determined with the knowledge of the drift velocity. In each chamber, track segments are reconstructed using a linear fit to the hits, and are used for the offline reconstruction of the muon tracks [8]. For triggering purposes, the DT Local Trigger algorithm searches for aligned hits, called trigger segments, in each chamber, using dedicated electronics and algorithms that are independent of the TDC track fitting.

2.2 The Drift-Tube Local Trigger

The DT Local Trigger system and its performance are described in detail in Refs. [4, 9, 10]. Dedicated adjustments to the configuration of the DT trigger were needed to provide high efficiency for cosmic ray muons, which have a different origin, direction, and timing compared to muons from proton-proton collisions [11]. In this section, only the main functionalities and characteristics are summarized. The trigger segments are found separately in the transverse plane $x-y$ (called ϕ view) and in the plane that contains the z direction (called θ view).

The maximum drift time in the DT system is almost 400 ns, which is much longer than the 25 ns interval that separates two consecutive collisions. Therefore, the trigger system must first associate each trigger segment to the correct bunch crossing (BX). For each BX the trigger system provides up to two trigger segments per chamber in the ϕ view, and one in the θ view. In the ϕ view, each trigger segment is associated with the following quantities: the BX, at which the corresponding muon candidate was produced; the position and direction in the local coordinate system of the chamber; a quality word describing how many aligned DT hits were found; and a bit flagging the segment as a first or second candidate, ordered according to their assigned quality, for that BX. One set of such quantities is called a “trigger primitive”.

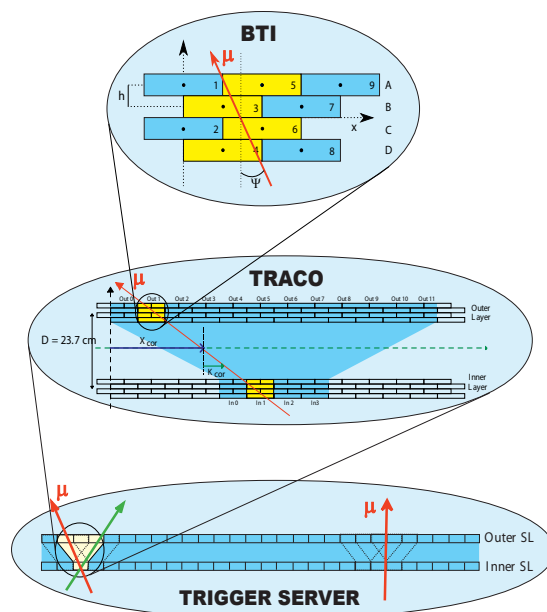


Figure 2: The main components of the DT Local Trigger in the ϕ view of a muon chamber. The BTIs detect hit alignments within each superlayer, the TRACOs search for a proper matching between superlayers, and the Trigger Server selects the best two candidates in the chamber and applies a ghost-suppression algorithm.

Trigger segments in the θ view are issued if there are three or four aligned hits in the corresponding superlayer. The θ trigger primitive includes the assigned BX, a word defining the

location in the chamber, and its quality word. During LHC operation, the system in the θ view will be configured to accept only trigger segments pointing to the interaction region. This condition was not applied for data taking with cosmic rays.

The trigger algorithm that provides the trigger primitives in the ϕ view works in three logical steps that are sketched in Fig. 2. For every BX, the Bunch and Track Identifiers (BTIs) search for track segment candidates made of three or four aligned DT hits within a superlayer. Each candidate is processed by the Track Correlators (TRACOs), which search for a proper angular matching between the candidates from the two superlayers in each chamber. TRACO candidates are then sent to the Trigger Server, which performs a ghost-suppression mechanism and then selects for each BX the two trigger primitives with highest quality. The quality is defined according to the number of aligned hits in the trigger segment. An alignment of hits in a superlayer is labeled “High” (H) or “Low” (L) if it includes four or three DT hits, respectively. The quality of a trigger segment in the ϕ view is labeled HH, HL, or LL if a matching (correlation), both in angle and BX, is found between the segments of the two superlayers. In this case the trigger segments are called “correlated”. If no correlation is found, and four aligned hits are detected in the inner (outer) superlayer of the chamber (where inner and outer are defined according to their distance from the center of the CMS detector), the segment quality is labeled as HI (HO).

The DT Local trigger is designed for triggering on particles produced synchronously with the bunch crossing signal. One of the effects of the random arrival time of the cosmic muons is the production of spurious uncorrelated trigger segments with wrong bunch crossing assignment. Therefore, to reduce the rate of such spurious triggers, the DT Local Trigger was configured such that the presence of a θ trigger segment was required to accept uncorrelated H-quality triggers in the ϕ view. At the LHC, where muons are synchronously produced with the bunch crossing signal, spurious triggers will be largely suppressed, so that the trigger configuration will be relaxed to accept also uncorrelated L-quality triggers.

The ghost-suppression mechanism is performed to discard additional trigger candidates attributable to false signals (“ghosts”). The false trigger segments mostly arise from the fact that adjacent TRACO units share a common group of DT cells, and a hit alignment can be found twice. The segment selection and ghost-suppression algorithms are flexible and can be configured to match various experimental conditions, such as the presence of groups of noisy or disconnected DT cells in a chamber.

The position and angle parameters of the trigger segment, named Φ and Φ_b respectively, are illustrated in Fig. 3, together with the angle ψ that defines the inclination of the trigger segment with respect to the direction perpendicular to the chamber plane. The parameter Φ is determined by the position of the trigger segment with respect to the center of the chamber, whereas the quantity Φ_b is the angle between the direction of the trigger segment and the straight line from the interaction point to the segment position.

The data from the four Trigger Server units of every muon sector are sent to the Regional Trigger [12], which independently performs the matching between trigger segments in the ϕ and θ views, using two different systems: the Phi Track Finder and the Eta Track Finder, respectively. In the data analysed for this study the Eta Track Finder was not yet operational. The matching of segments between chambers is performed by the Phi Track Finder using configurable look-up tables, which define the range, in terms of position and angle, where a valid extrapolation of a trigger segment from one chamber to another is expected. The Phi Track Finder extrapolation mechanism was not used during the data taking with cosmic ray muons in order to maximize the geometrical acceptance. The Phi Track Finder processed data within one sector

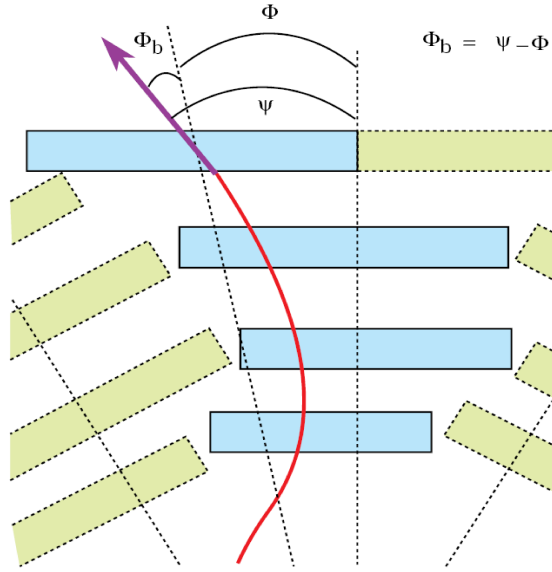


Figure 3: Definition of the Φ and Φ_b parameters provided by the DT Local Trigger, shown for the outermost muon chamber. The angle ψ represents the inclination of the trigger segment with respect to the direction perpendicular to the chamber plane. The angle Φ is defined with respect to the center of the chamber.

or two neighboring sectors, by searching for a signal coincidence in at least two chambers. Up to four candidates, ordered according to their transverse momenta, are selected and forwarded to the Global Muon Trigger, where they are combined with muon-trigger candidates from RPCs and CSCs [4]. During data taking with cosmic rays, a Level-1 trigger rate of about 240 Hz was passed from the Phi Track Finder to the Global Muon Trigger.

The DT Local Trigger signals from the various chambers must arrive synchronously at the Regional Trigger, and a dedicated synchronization procedure was developed for triggering with cosmic rays. The time taken by the particles traversing the detector from top to bottom depends on the track incident angle, and is approximately 50 ns for cosmic muons traversing both sectors 4 and 10. To synchronize the DT trigger system, the latency of the trigger signals of the chambers in the upper sectors was increased up to a maximum delay time of 50 ns, which corresponds to two bunch crossings. The delays for each individual chamber were obtained with data from dedicated synchronization runs by examining the bunch crossing distribution of the trigger segments from different detector regions with respect to a reference sector. This allowed the synchronization of all chambers to be within a fraction of a bunch crossing, regardless of the direction and the position of the incoming particle.

2.3 The Event Selection

Unless explicitly mentioned, the results shown in this paper are obtained using data collected with the CMS solenoid operating at 3.8 T. The data were collected in periods of stable DT operation. No requirements on the status of the other CMS detectors and their participation in the data taking are applied to the event selection, except when explicitly mentioned. The sample used for the analysis corresponds to approximately 10 million events. This is large enough to make statistical uncertainties negligible for the measurements performed.

The trigger and data acquisition are synchronized with a 40 MHz signal replicating the LHC BX

frequency. The Level-1 Trigger signal requires the coincidence, at the same BX, of at least two trigger primitives from two chambers of the same sector or of two adjacent sectors. To avoid any bias in the event selection, it is required that at least two chambers distinct from the one under investigation have provided trigger primitives. This guarantees that the event is selected by the Level-1 Trigger independently of the chamber under investigation. To measure the trigger efficiency in a chamber, the presence of a local track segment reconstructed with at least 7 out of 8 TDC hits in the ϕ view is also required. The radial angle of the track segment must be in the range $|\psi| < 30^\circ$, to stay within the TRACO angular acceptance. To remove events with two or more muon tracks in the same chamber, at most 12 TDC hits are allowed in the ϕ view of the chamber under investigation. The efficiency of the DT Local Trigger in the chamber is defined as the fraction of the selected events that have an associated trigger primitive in the chamber, in the same or in any of the two adjacent BXs. This definition of efficiency allows the measurement of the effective net trigger capability, excluding the geometrical acceptance and the DT cell efficiency. This event selection is employed for the analysis described in this paper, except where explicitly stated otherwise.

3 Performance of the DT Local Trigger

Muons produced in LHC collisions will cross each DT chamber at a well defined time with respect to the signal of the BX clock, with a jitter of a few nanoseconds, due to the different path lengths in the magnetic field. The BTI electronics will be properly synchronized with the arrival time of the particles to perform the best hit alignment [13, 14]. However, cosmic ray muons traverse the detector at arbitrary times with respect to the 40 MHz signal that simulates the BX clock. Taking the signal of the BX clock as a time reference, the BTI is configured to detect hit alignments in the most efficient way in a time range that is about 10 ns wide. Therefore, only muons arriving within the 10 ns time window will be correctly identified by the trigger, while outside this time window the efficiency of the BTI to find aligned hits is degraded.

3.1 Trigger Efficiency

To illustrate the effect of the random arrival time of the cosmic rays on the performance measurements presented in this paper, Fig. 4 shows the DT Local Trigger efficiency as a function of the arrival time of the muon with respect to the global time reference t_{Trig} . The quantity t_{Trig} represents the value to be subtracted from the time measured by the TDC (called t_{Digi}) to correct for the trigger latency and for differences in the propagation time of the signals in the system. The determination of t_{Trig} is described in Ref. [15], and it is performed by fitting the position of the rising edge of the t_{Digi} distribution separately in each superlayer. The arrival time with respect to t_{Trig} is individually computed for every muon and event, by performing a linear fit to the TDC hits in the chamber. The arrival time is a free parameter of the fit, and it is determined, event-by-event, as the time shift to be added to t_{Trig} giving the best spatial resolution for every event by achieving the best track-segment fit [16]. This shift represents the time offset at which the muon traversed the chamber with respect to the reference time t_{Trig} , which is the mean arrival time averaged over many events.

Figure 4 shows that the DT Local Trigger efficiency is not constant as a function of the arrival time of the particle, in particular for trigger segments of HH quality, but it is maximal and flat in a region approximately 10 ns wide. To first order, the efficiency has a periodicity of 25 ns, which is the time difference between two consecutive BXs. As the events selection requires the time coincidence of trigger segments in at least two chambers, uncertainties in their relative synchronization, which was typically of the order of a fraction of a BX during the period of

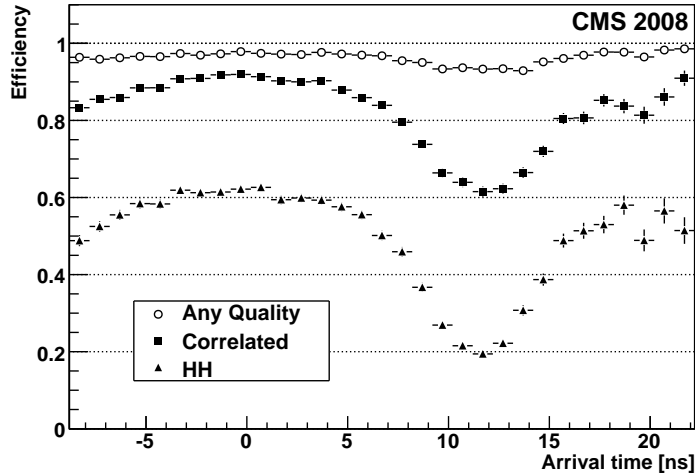


Figure 4: Efficiency of the DT Local Trigger as a function of the muon arrival time in the chamber, defined with respect to the t_{Trig} time reference. Results for a chamber of type MB1 are shown as an example, for various types of trigger quality.

data taking, can bias the measured arrival time of the muons, thus resulting in an imperfect periodicity of the efficiency curve. The time dependence of the efficiency reflects the fact that the trigger system is optimized for muons arriving in the time range corresponding to the flat-top region of Fig. 4. For LHC operation, the trigger timing will be adjusted so that muons from collisions will traverse the detector within this time range. For the tests with cosmic ray muons, however, this results in an overall degradation of the average performance of the DT Local Trigger compared to the expectations for the LHC and the results with bunched-beam tests, in terms of efficiency, quality of the trigger primitives, and BX identification.

In the 10 ns flat-top region, where the trigger system is well synchronized with the incoming particles, the DT Local Trigger efficiency is approximately 0.60 for triggers of HH quality, 0.90 for correlated triggers, and 0.97 for any trigger quality. These values are consistent with previous measurements at bunched-beam tests [9, 10], as well as with the technical specifications required for efficient triggering with particle collisions [4].

The average DT Local Trigger efficiencies obtained using all cosmic ray muons, regardless of their arrival time with respect to the reference time t_{Trig} , are 0.95 for triggers of any quality, 0.80 for correlated triggers, and 0.48 for triggers of HH quality. These values are lower than the values reached in the plateau of maximum efficiency shown in Fig. 4, where the performance of the system is optimal. They have a spread of 0.02 among the chambers, mostly caused by the different angles of incidence of the cosmic rays on the chambers and by a few malfunctioning trigger devices. The few chambers with major hardware or read-out problems are not taken into account in the computation. These problems were fixed during the detector shutdown at the end of 2008.

The results on the DT Local Trigger efficiency are cross-checked using an independent event selection that does not explicitly require the presence of DT hits in the chamber under study. For this purpose, events triggered by the RPCs are selected. In such events, muon tracks are subsequently reconstructed using the DT hits in the muon barrel and CSC hits in the endcaps. The tracks are extrapolated along the detector, and required to cross the chamber under study in its active region, without any requirement on the presence of DT hits in that chamber. The

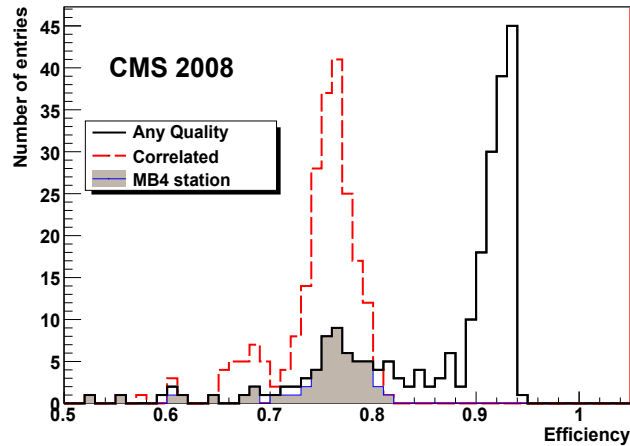


Figure 5: Distribution of the DT Local Trigger efficiency in the ϕ view of the muon chambers, for events selected by the RPC trigger. Each entry corresponds to one barrel chamber. Results for any trigger quality and for correlated triggers are shown. The shaded histogram represents the results for station type MB4, for which only correlated triggers are provided.

chamber is considered efficient if there is a trigger segment in the ϕ view, in the same or in any of the two adjacent BXs. In order to remain within the geometrical acceptance of the trigger, only tracks with an angle of incidence $|\psi| < 30^\circ$ were considered. Figure 5 shows the distribution of the DT Local Trigger efficiency measured for these events. Each entry represents one muon chamber. Results are shown for any trigger quality and for correlated triggers. Results for station type MB4, for which only correlated triggers are provided, are shown separately. In contrast to the previously described measurement, this definition of the DT Local Trigger efficiency includes effects of geometrical acceptance at the edges of the chambers, cell inefficiency, dead channels, and hardware failures. Therefore, the measured values are on average a few percent lower than the ones previously reported. For triggers of any quality the efficiency distribution has a maximum at 95%. Values below 70% are due to read-out or hardware problems, which have been fixed during the detector shutdown at the end of 2008. For correlated triggers, the efficiencies below 70% are related to chambers oriented vertically in the detector (sectors 1 and 7). In this case, given the angular distribution of cosmic rays, there is a high probability to fail the correlation between superlayers near the edges of the chambers. In this detector region the low efficiency is partially recovered if trigger segments of any quality are accepted, and in this case it reaches values between 80% and 90%.

The DT Local Trigger efficiency as a function of the incidence angle $|\psi|$ is also measured, for trigger segments of any quality. In this case the requirement on the incidence angle of the track, $|\psi| < 30^\circ$, is removed, and the efficiency value is averaged over all chambers, with the exclusion of sectors 1 and 7. The results, reported in Fig. 6, are in agreement with previous test beam measurements [9] and show that the trigger efficiency has a constant plateau for tracks with inclination up to about 35° , and it decreases by a factor of 2 at the maximum BTI angular acceptance of 45° . This corresponds, in the case of LHC collisions, to full trigger efficiency for tracks with transverse momenta exceeding 3 GeV/c.

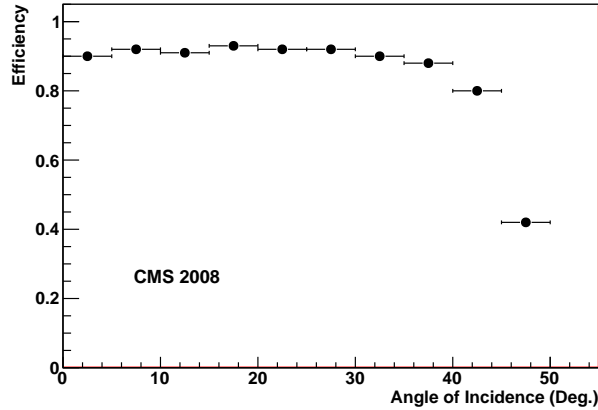


Figure 6: Average DT Local Trigger efficiency in the ϕ view of the muon chambers for trigger segments of any quality, as a function of the angle of incidence $|\psi|$ of the muon tracks.

3.2 Bunch Crossing Identification

The performance of the BX identification is measured by comparing the assigned bunch crossing in the chamber under study, called “trigger BX”, with respect to the BX defined by the coincidence of the other two trigger segments in the same sector, called “expected BX”. The difference between the “expected BX” and the “trigger BX” is shown in Fig. 7 for different trigger qualities. The data from a chamber of type MB1 in sector 4 are used as an example. The results are similar for the other chambers in the detector. The events for which the difference between the “expected BX” and the “trigger BX” is zero have a correct BX identification. The distributions, normalized to unity, show that, even in the difficult environment of cosmic rays, triggers of HH quality provide correct BX identification in 82 % of the cases. The distribution is affected by imperfect synchronization between the chambers during data taking. The distribution is wider for poorer trigger quality. Because of a feature of the BTI system, the events with badly identified BX mainly populate the left-most part of the distribution for low-quality triggers, as they are trigger segments with wrong hit alignments that are typically produced later with respect to the correct BX. Such triggers are significantly suppressed in the case of quality type HH.

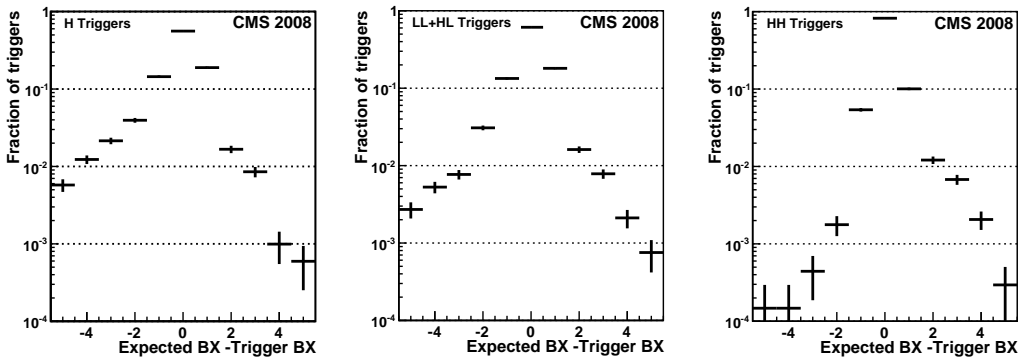


Figure 7: Distribution of the difference between the “expected BX” and the observed BX (“trigger BX”) of the trigger segment, in one chamber of type MB1 in sector 4, for different trigger qualities. The distributions are normalized to unity.

In bunched-beam tests the BX identification for trigger segments of quality HH was close to 100% [9, 10]. In the present analysis, the degraded performance of the BX identification is explained by the timing characteristics of the cosmic rays already discussed. Events selected with the optimal arrival time of the muon tracks (as discussed in section 3.1) show that the BX identification capability for triggers of HH quality approaches 100%, thus matching the design expectations for proton-proton collisions. This can be seen in Fig. 8, which shows the distribution of the arrival time of the muon tracks (in the same chamber used for Fig. 4), for events with a trigger segment of any quality (left) and for quality type HH (right). The distributions for trigger segments with correct BX assignment (“expected BX” equal to “trigger BX”) and wrong BX assignment are shown separately. In the region approximately ± 5 ns wide around zero, where the timing of the trigger system is optimized (as discussed for the results of Fig. 4), the wrongly timed triggers of any quality contribute only marginally, and they can be completely neglected in the case of trigger segments of HH quality.

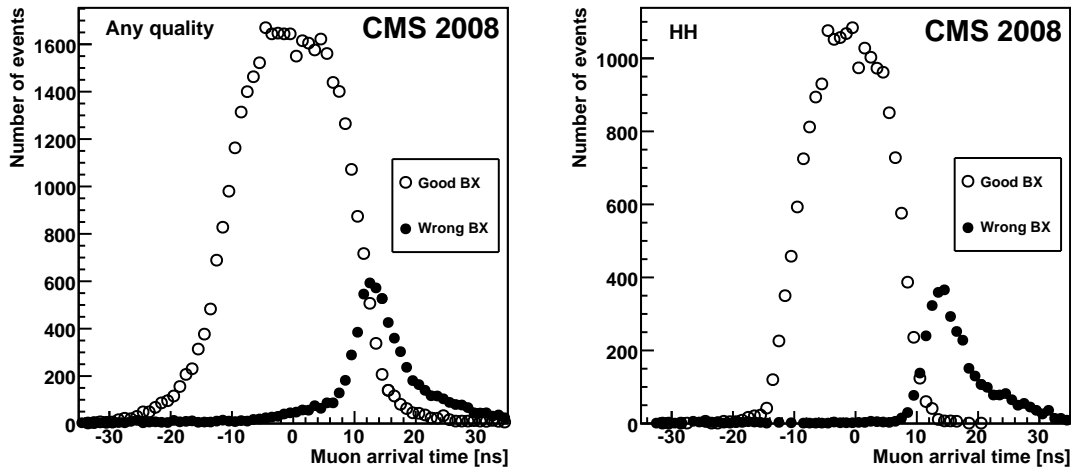


Figure 8: Left: distribution of the muon arrival time, for trigger segments of any quality. Right: distribution of the muon arrival time for trigger segments of HH quality. Events with correct and wrong BX identification are shown separately. Results for a chamber of type MB1 in sector 4 are shown as an example.

3.3 False Dimuon Trigger Rate

The DT Local Trigger provides up to two trigger segments for any BX in the ϕ view of each chamber. This feature was introduced to maximize the trigger efficiency for nearby muons. On the other hand, a ghost suppression mechanism is implemented to reject false trigger pairs that originate from a single muon crossing the detector. As the dimuon production rate above any given transverse momentum threshold is expected to be approximately 1% of the single muon rate at the LHC [4], the rate of false Level-1 dimuon triggers must be well below 1%. With cosmic rays the fraction of double triggers over single triggers provided in a single chamber at the same BX, averaged over all the chambers of type MB1, MB2, and MB3, is 0.03 ± 0.01 . The DT Local Trigger in station type MB4 provides a lower fraction of double triggers, namely 0.012 ± 0.005 , since only correlated trigger segments are provided by this station type. The uncertainty reflects the observed spread of values among the various chambers, due to systematic effects like noisy channels, or different angles of incidence of the cosmic rays. The results are consistent with test beam measurements [9, 10]. The false dimuon Level-1 trigger rate in

the barrel region is further suppressed, as the matching of at least two segments in two different chambers is required to form a trigger candidate, and as a further selection is applied by the Global Muon Trigger. The measured false dimuon trigger rate per chamber is significantly smaller compared to the assumptions made in Ref. [4]. Hence, the false dimuon Level-1 rate in the barrel region is estimated to be below the 0.1 % reported in Ref. [4], which is at least one order of magnitude smaller than the real dimuon rate and can, therefore, be neglected.

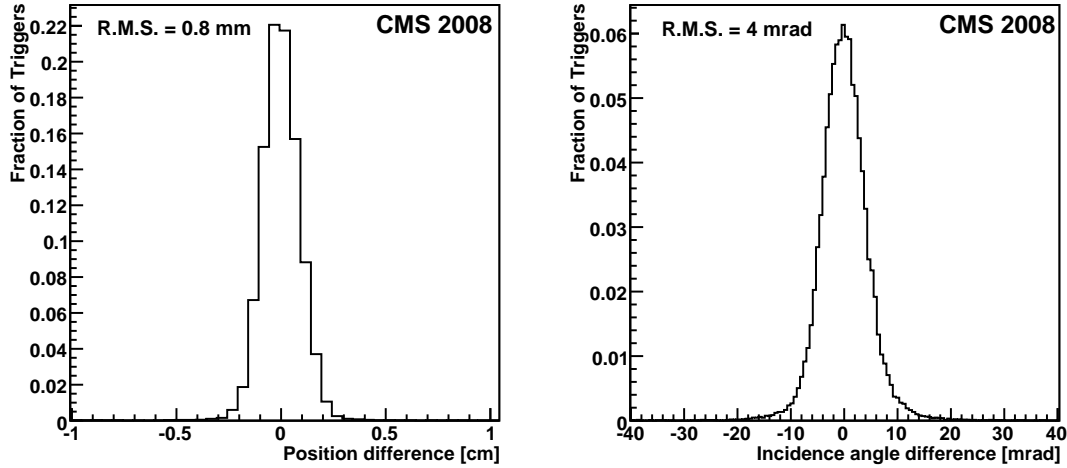


Figure 9: Left: distribution of the difference between the position of the local track segment and the trigger segment. Right: distribution of the difference between the incidence angle measured by the local track segment and the trigger segment. Results are shown for a chamber of type MB1.

3.4 Position and Angular Resolution

The track segments obtained by fitting the TDC information in each chamber and used for offline muon reconstruction provide an accurate determination of the position and the incidence angle of the muon in the chamber independent of the trigger output. These quantities are compared with the corresponding information assigned by the DT Local Trigger to the trigger segments, Φ and Φ_b . Figure 9 (left) shows the distribution of the difference between the position computed by the reconstructed track segment and by the trigger segment for a chamber of type MB1 taken as an example. The RMS of the distribution is 0.8 mm. This provides an estimate of the position resolution of the trigger segment, which is the same for every station type. This measurement is in agreement with previous test beam results [9]. The uncertainty related to the track position measurement is neglected.

A similar study is performed on the track incidence angle ψ . Figure 9 (right) shows the distribution of the difference between the incidence angle of the reconstructed track and the trigger segment. The RMS of the distribution is 4 mrad. Taking into account the slight reduction of the angular resolution arising from the timing characteristics of the cosmic rays, the resolution is in agreement with the value of 3 mrad obtained in previous test beam measurements [9]. The result guarantees that the expected performance in terms of position and transverse momentum resolution at the output of the Level-1 trigger will be achieved for collision data taking [4].

3.5 Effect of the Magnetic Field

In station type MB1 of the wheels +2 and -2, the magnetic field is expected to affect the drift-path lengths such that the maximum drift time is increased by $\mathcal{O}(10 \text{ ns})$ [17]. A variation of the maximum drift time, which corresponds to an apparent change of the drift velocity, could degrade the DT Local Trigger performance, affecting in particular the BX identification. A sample of approximately 5 million events collected with no magnetic field is used to study this effect. The means of the BX distributions determined by the DT Local Trigger in a chamber (obtained as in Fig. 7) are compared for data taken with and without the magnetic field.

Some corrections are applied to compare the results obtained from the two data sets. As muons are bent by the magnetic field, the timing of the trigger signals between the various chambers and sectors is slightly affected because of the different path length, especially for low momentum particles. In addition, some further adjustments in the synchronization between the various sectors were performed between the two data taking periods. Therefore, a direct comparison of the means of the BX distributions obtained in the two conditions is biased by these systematic effects. As in station type MB4 the effect of the magnetic field on the drift velocity is expected to be negligible, it is assumed that in this case any deviation from zero observed in the difference of the BX distributions is entirely due to the systematic effects. Results for station type MB4 are then set to zero, separately in each sector, and the results for the other stations are shifted by the same amount to correct for the systematic effects.

Figure 10 shows the difference between the means of the BX distributions, with and without the magnetic field, as a function of the wheel number for different station types, after the correction procedure described above. The results are averaged over the various sectors, and only statistical uncertainties are shown in the figure. Small deviations from zero are observed in all stations and wheels, and they are partially due to the aforementioned systematic uncertainties, which could not be completely suppressed. The largest deviation from zero is observed in MB1, at the wheels +2 and -2, where the magnetic field is indeed expected to have the largest effect on BX identification. Comparing results with and without the magnetic field, the maximum average BX displacement is 0.1 units of a BX, corresponding to about 3 ns. This shift is much smaller than 25 ns, which is the time between two consecutive BXs, and thus it cannot significantly affect the performance of the trigger [17].

A study of the BX displacement as a function of the position of the trigger candidate along the z coordinate shows that the BX assignment is fairly constant across the muon chambers, increasing at the edges with the maximum value of 5 ns, which is sufficiently small compared to 25 ns. Consequently it is possible to configure the BTIs with the same value of the drift-velocity parameter in each chamber, regardless of its location in the detector or the magnetic field.

The comparison between events recorded with and without the magnetic field is used to study the effect of the field on the position and angular resolution of the trigger segments. The results show that the position and direction determination by the DT Local Trigger is not affected by the presence of the magnetic field. The comparison of data taken with and without the magnetic field also shows that the magnetic field does not affect the trigger efficiency, except in station MB1 of the wheels +2 and -2 where the fraction of correlated triggers is decreased by less than 2%.

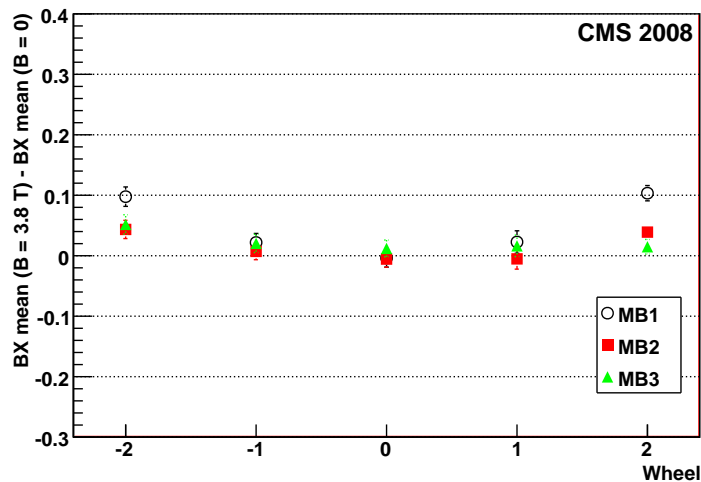


Figure 10: Difference between the means of the BX distributions determined by the DT Local Trigger with and without magnetic field, in units of BX, as a function of the wheel number, for MB1, MB2 and MB3 station types.

4 Comparison with the Emulator

A detailed simulation of the DT Local Trigger selection algorithm is implemented in the CMS software framework, and is part of the emulator program that reproduces the output of the entire Level-1 trigger. The emulator processes the signals from the drift cells: for each cell the difference $t_{\text{Digi}} - t_{\text{Trig}}$ is computed and sent as input to the emulator. The quantity received as input by the trigger electronics is not exactly the same as $t_{\text{Digi}} - t_{\text{Trig}}$, although its physical meaning is the same. In fact, the BTIs are directly linked to the wires of the DT chamber, receiving discriminated signals on the on-board electronics, while the quantity t_{Digi} and the pedestal parameter t_{Trig} are determined by the TDCs (which have a different hardware connection to the DT cells with respect to the BTIs) and by an offline analysis, respectively. This makes the exact data-emulator agreement impossible by design. Discrepancies between data and emulation, on an event-by-event comparison, are mostly observed in the quality of the trigger primitives. Even considering this intrinsic limitation, an event-by-event comparison shows that, among all the trigger primitives provided by the trigger electronics, more than 90% are perfectly reproduced by the emulator in all their characteristics. If the comparison between data and emulator is performed on a statistical basis rather than event-by-event, the differences between data and emulator largely compensate, and the agreement approaches 100%. This can be seen in Fig. 11, which shows the comparison of the distribution of the trigger quality for station types MB1 and MB4.

The emulator program assumes a perfectly working trigger system, so that any significant discrepancy with the data is an indication either of malfunctioning electronics or mis-configuration. On the other hand, dead cells, high-voltage problems, noisy cells, or any other malfunctions affecting the presence of the digitized information from the TDCs, but not related to the trigger devices, are always reproduced by the emulation, resulting in a very good matching with the data. Therefore, the emulator is a very powerful tool for use during data taking for diagnosing problems that are related to the trigger system.

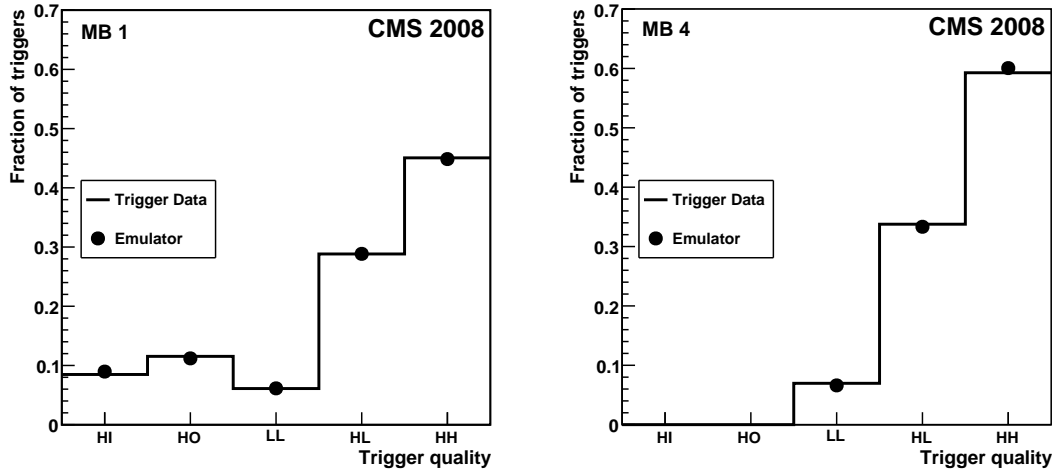


Figure 11: Distribution of the quality of the trigger segments, for data and emulation, for station types MB1 (left) and MB4 (right).

5 Conclusions

The muon Local Trigger based on the drift-tube detector of the CMS experiment has been extensively tested during the commissioning of the apparatus using cosmic rays. Cosmic rays traverse the detector at arbitrary times and with different directions compared to particles produced in LHC collisions, for which the muon trigger was designed. Therefore, the system performance is degraded with respect to the expectations for the LHC, or if compared with measurements previously performed with bunched beams. Nevertheless, the device operated in a very efficient and reliable way. An overall efficiency of 95 % is obtained, and 48 % of the trigger segments are of the best possible quality. An accurate measurement of the trigger efficiency as a function of the timing of the system shows that, in the time window where the trigger electronics is properly synchronized with the arriving muon, as it will be the case for particles produced at LHC collisions, the DT Local trigger efficiency is 97 % for any trigger quality. The performance of the BX identification reaches 100 % when a correction for the arbitrary arrival time of cosmic ray muons is performed. The rate of false double triggers for single muons is about 1.5–3.0 % of the single muon triggers in one chamber. As the coincidence of trigger segments in at least two chambers is needed by the Phi Track Finder to reconstruct a trigger candidate, and as a further selection is applied by the Regional and the Global Muon Trigger, the false dimuon trigger rate is expected to be at least one order of magnitude smaller than the real dimuon rate expected from LHC collisions at any transverse momentum threshold. The position and angular resolution of the trigger segments is 0.8 mm and 4 mrad, respectively. This performance allows the trigger system to achieve the position and transverse momentum resolution needed for efficient operation with collisions. The magnetic field has a negligible impact on the bunch crossing identification, on the position and angular resolution, and on the trigger efficiency, even in the detector regions where the effect should be largest. Trigger data were also successfully cross-checked with the emulator. Although a perfect event-by-event agreement with the data is impossible by design, more than 90 % of the trigger primitives are perfectly reproduced by the emulator in all their characteristics. This makes the emulator a powerful tool for diagnosing problems related to the trigger system during data taking.

Acknowledgements

We thank the technical and administrative staff at CERN and other CMS Institutes, and acknowledge support from: FMSR (Austria); FNRS and FWO (Belgium); CNPq, CAPES, FAPERJ and FAPESP (Brazil); MES (Bulgaria); CERN; CAS, MoST and NSFC (China); COLCIENCIAS (Colombia); MSES (Croatia); RPF (Cyprus); Academy of Sciences and NICPB (Estonia); ME, HIP and Academy of Finland (Finland); CEA and CNRS/IN2P3 (France); BMBF and DESY (Germany); BMBF, DFG and HGF (Germany); GSRT (Greece); OTKA and NKTH (Hungary); DAE and DST (India); IPM (Iran); SFI (Ireland); INFN (Italy); NRF (Korea); LAS (Lithuania); CINVESTAV, CONACYT, SEP and UASLP-FAI (Mexico); PAEC (Pakistan); SCSR (Poland); FCT (Portugal); JINR (Armenia, Belarus, Georgia, Ukraine, Uzbekistan); MST and MAE (Russia); MSTDS (Serbia); MCINN and CPAN (Spain); Swiss Funding Agencies (Switzerland); NSC (Taipei); TUBITAK and TAEK (Turkey); STFC (United Kingdom); DOE and NSF (USA). Individuals have received support from the Marie-Curie IEF program (European Union); the Leventis Foundation; the A. P. Sloan Foundation; and the Alexander von Humboldt Foundation

References

- [1] CMS Collaboration, “The CMS Experiment at the CERN LHC”, *JINST* **0803**: (2008) 08004. doi:10.1088/1748-0221/2/08/S08004.
- [2] J. Evans and B. P., “LHC Machine”, *JINST* **3** (2008) 08004. doi:10.1088/1748-0221/3/08/S08001.
- [3] CMS Collaboration, “Commissioning of the CMS Experiment and the Cosmic Run at Four Tesla”, arXiv:0911.4845v1.
- [4] CMS Collaboration, “The Level-1 Trigger, Technical Design Report”, *CERN/LHCC 2000-038* (2000).
- [5] CMS Collaboration, “CMS Data Processing Workflow During an Extended Cosmic Ray Run”, arXiv:0911.4842v1.
- [6] CMS Collaboration, “The Muon Project, Technical Design Report”, *CERN/LHCC 1997-32* (1997).
- [7] CMS Collaboration, “CMS Physics TDR: Volume 1, Detector Performance and Software”, *CERN/LHCC 2006-001* (2006).
- [8] CMS Collaboration, “Performance of the CMS Drift-Tube Chambers with Cosmic Rays”, arXiv:0911.4855v1.
- [9] P. Arce et al., “Bunched beam test of the CMS drift tubes local muon trigger”, *Nucl. Instr. and Meth.* **A534** (2004) 441. doi:10.1016/j.nima.2004.06.169.
- [10] M. Aldaya et al., “Results of the first integration test of the CMS drift tubes muon trigger”, *Nucl. Instr. and Meth.* **A579** (2007) 951. doi:10.1016/j.nima.2007.06.007.
- [11] CMS Collaboration, “Performance of the CMS Level-1 Trigger during Commissioning with Cosmic Rays”, arXiv:0911.5422v1.
- [12] J. Ero et al., “The CMS Drift-Tube Trigger Track Finder”, *JINST* **3** (2008) P08004. doi:10.1088/1748-0221/2/08/P08006.

-
- [13] M. Aldaya et al., “Fine synchronization of the muon drift tubes local trigger”, *Nucl. Instr. and Meth.* **A564** (2006) 169. doi:10.1016/j.nima.2006.04.046.
- [14] CMS Collaboration, “Fine Synchronization of the CMS Muon Drift-Tube Local Trigger Using Cosmic Rays”, arXiv:0911.4904v1.
- [15] CMS Collaboration, “Calibration of the CMS Drift-Tube Chambers and Measurement of the Drift Velocity with Cosmic Rays”, arXiv:0911.4895v1.
- [16] M. Benettoni et al., “CMS DT Chambers: Optimized Measurement of Cosmic Rays Crossing Time in Absence of Magnetic Field”, *CMS Note* **2008-017** (2008).
- [17] M. Aguilar-Benitez et al., “Study of magnetic field effects in drift tubes for the barrel muon chambers of the CMS detector at the LHC”, *Nucl. Instr. and Meth.* **A416** (1998) 243. doi:10.1016/S0168-9002(98)00681-0.

A The CMS Collaboration

Yerevan Physics Institute, Yerevan, Armenia

S. Chatrchyan, V. Khachatryan, A.M. Sirunyan

Institut für Hochenergiephysik der OeAW, Wien, Austria

W. Adam, B. Arnold, H. Bergauer, T. Bergauer, M. Dragicevic, M. Eichberger, J. Erö, M. Friedl, R. Frühwirth, V.M. Ghete, J. Hammer¹, S. Hänsel, M. Hoch, N. Hörmann, J. Hrubec, M. Jeitler, G. Kasieczka, K. Kastner, M. Krammer, D. Liko, I. Magrans de Abril, I. Mikulec, F. Mittermayr, B. Neuherz, M. Oberegger, M. Padrta, M. Pernicka, H. Rohringer, S. Schmid, R. Schöfbeck, T. Schreiner, R. Stark, H. Steininger, J. Strauss, A. Taurok, F. Teischinger, T. Themel, D. Uhl, P. Wagner, W. Waltenberger, G. Walzel, E. Widl, C.-E. Wulz

National Centre for Particle and High Energy Physics, Minsk, Belarus

V. Chekhovsky, O. Dvornikov, I. Emeliantchik, A. Litomin, V. Makarenko, I. Marfin, V. Mossolov, N. Shumeiko, A. Solin, R. Stefanovitch, J. Suarez Gonzalez, A. Tikhonov

Research Institute for Nuclear Problems, Minsk, Belarus

A. Fedorov, A. Karneyeu, M. Korzhik, V. Panov, R. Zuyevski

Research Institute of Applied Physical Problems, Minsk, Belarus

P. Kuchinsky

Universiteit Antwerpen, Antwerpen, Belgium

W. Beaumont, L. Benucci, M. Cardaci, E.A. De Wolf, E. Delmeire, D. Druzhkin, M. Hashemi, X. Janssen, T. Maes, L. Mucibello, S. Ochesanu, R. Rougny, M. Selvaggi, H. Van Haevermaet, P. Van Mechelen, N. Van Remortel

Vrije Universiteit Brussel, Brussel, Belgium

V. Adler, S. Beauceron, S. Blyweert, J. D'Hondt, S. De Weirtdt, O. Devroede, J. Heyninck, A. Kalogeropoulos, J. Maes, M. Maes, M.U. Mozer, S. Tavernier, W. Van Doninck¹, P. Van Mulders, I. Villella

Université Libre de Bruxelles, Bruxelles, Belgium

O. Bouhali, E.C. Chabert, O. Charaf, B. Clerbaux, G. De Lentdecker, V. Dero, S. Elgammal, A.P.R. Gay, G.H. Hammad, P.E. Marage, S. Rugovac, C. Vander Velde, P. Vanlaer, J. Wickens

Ghent University, Ghent, Belgium

M. Grunewald, B. Klein, A. Marinov, D. Ryckbosch, F. Thyssen, M. Tytgat, L. Vanelderen, P. Verwilligen

Université Catholique de Louvain, Louvain-la-Neuve, Belgium

S. Basegmez, G. Bruno, J. Caudron, C. Delaere, P. Demin, D. Favart, A. Giammanco, G. Grégoire, V. Lemaitre, O. Militaru, S. Oryn, K. Piotrkowski¹, L. Quertenmont, N. Schul

Université de Mons, Mons, Belgium

N. Bely, E. Daubie

Centro Brasileiro de Pesquisas Fisicas, Rio de Janeiro, Brazil

G.A. Alves, M.E. Pol, M.H.G. Souza

Universidade do Estado do Rio de Janeiro, Rio de Janeiro, Brazil

W. Carvalho, D. De Jesus Damiao, C. De Oliveira Martins, S. Fonseca De Souza, L. Mundim, V. Oguri, A. Santoro, S.M. Silva Do Amaral, A. Sznajder

Instituto de Fisica Teorica, Universidade Estadual Paulista, Sao Paulo, Brazil

T.R. Fernandez Perez Tomei, M.A. Ferreira Dias, E. M. Gregores², S.F. Novaes

Institute for Nuclear Research and Nuclear Energy, Sofia, Bulgaria

K. Abadjiev¹, T. Anguelov, J. Damgov, N. Darmanov¹, L. Dimitrov, V. Genchev¹, P. Iaydjiev, S. Piperov, S. Stoykova, G. Sultanov, R. Trayanov, I. Vankov

University of Sofia, Sofia, Bulgaria

A. Dimitrov, M. Dyulendarova, V. Kozhuharov, L. Litov, E. Marinova, M. Mateev, B. Pavlov, P. Petkov, Z. Toteva¹

Institute of High Energy Physics, Beijing, China

G.M. Chen, H.S. Chen, W. Guan, C.H. Jiang, D. Liang, B. Liu, X. Meng, J. Tao, J. Wang, Z. Wang, Z. Xue, Z. Zhang

State Key Lab. of Nucl. Phys. and Tech., Peking University, Beijing, China

Y. Ban, J. Cai, Y. Ge, S. Guo, Z. Hu, Y. Mao, S.J. Qian, H. Teng, B. Zhu

Universidad de Los Andes, Bogota, Colombia

C. Avila, M. Baquero Ruiz, C.A. Carrillo Montoya, A. Gomez, B. Gomez Moreno, A.A. Ocampo Rios, A.F. Osorio Oliveros, D. Reyes Romero, J.C. Sanabria

Technical University of Split, Split, Croatia

N. Godinovic, K. Lelas, R. Plestina, D. Polic, I. Puljak

University of Split, Split, Croatia

Z. Antunovic, M. Dzelalija

Institute Rudjer Boskovic, Zagreb, Croatia

V. Brigljevic, S. Duric, K. Kadija, S. Morovic

University of Cyprus, Nicosia, Cyprus

R. Fereos, M. Galanti, J. Mousa, A. Papadakis, F. Ptochos, P.A. Razis, D. Tsiakkouri, Z. Zinonos

National Institute of Chemical Physics and Biophysics, Tallinn, Estonia

A. Hektor, M. Kadastik, K. Kannike, M. Müntel, M. Raidal, L. Rebane

Helsinki Institute of Physics, Helsinki, Finland

E. Anttila, S. Czellar, J. Härkönen, A. Heikkinen, V. Karimäki, R. Kinnunen, J. Klem, M.J. Kortelainen, T. Lampén, K. Lassila-Perini, S. Lehti, T. Lindén, P. Luukka, T. Mäenpää, J. Nysten, E. Tuominen, J. Tuominiemi, D. Ungaro, L. Wendland

Lappeenranta University of Technology, Lappeenranta, Finland

K. Banzuzi, A. Korpela, T. Tuuva

Laboratoire d'Annecy-le-Vieux de Physique des Particules, IN2P3-CNRS, Annecy-le-Vieux, France

P. Nedelec, D. Sillou

DSM/IRFU, CEA/Saclay, Gif-sur-Yvette, France

M. Besancon, R. Chipaux, M. Dejardin, D. Denegri, J. Descamps, B. Fabbro, J.L. Faure, F. Ferri, S. Ganjour, F.X. Gentit, A. Givernaud, P. Gras, G. Hamel de Monchenault, P. Jarry, M.C. Lemaire, E. Locci, J. Malcles, M. Marionneau, L. Millischer, J. Rander, A. Rosowsky, D. Rousseau, M. Titov, P. Verrecchia

Laboratoire Leprince-Ringuet, Ecole Polytechnique, IN2P3-CNRS, Palaiseau, France

S. Baffioni, L. Bianchini, M. Bluj³, P. Busson, C. Charlot, L. Dobrzynski, R. Granier de Cassagnac, M. Haguenaer, P. Miné, P. Paganini, Y. Sirois, C. Thiebaux, A. Zabi

Institut Pluridisciplinaire Hubert Curien, Université de Strasbourg, Université de Haute Alsace Mulhouse, CNRS/IN2P3, Strasbourg, France

J.-L. Agram⁴, A. Besson, D. Bloch, D. Bodin, J.-M. Brom, E. Conte⁴, F. Drouhin⁴, J.-C. Fontaine⁴, D. Gelé, U. Goerlach, L. Gross, P. Juillot, A.-C. Le Bihan, Y. Patois, J. Speck, P. Van Hove

Université de Lyon, Université Claude Bernard Lyon 1, CNRS-IN2P3, Institut de Physique Nucléaire de Lyon, Villeurbanne, France

C. Baty, M. Bedjidian, J. Blaha, G. Boudoul, H. Brun, N. Chanon, R. Chierici, D. Contardo, P. Depasse, T. Dupasquier, H. El Mamouni, F. Fassi⁵, J. Fay, S. Gascon, B. Ille, T. Kurca, T. Le Grand, M. Lethuillier, N. Lumb, L. Mirabito, S. Perries, M. Vander Donckt, P. Verdier

E. Andronikashvili Institute of Physics, Academy of Science, Tbilisi, Georgia

N. Djaoshvili, N. Roinishvili, V. Roinishvili

Institute of High Energy Physics and Informatization, Tbilisi State University, Tbilisi, Georgia

N. Amaglobeli

RWTH Aachen University, I. Physikalisches Institut, Aachen, Germany

R. Adolphi, G. Anagnostou, R. Brauer, W. Braunschweig, M. Edelhoff, H. Esser, L. Feld, W. Karpinski, A. Khomich, K. Klein, N. Mohr, A. Ostaptchouk, D. Pandoulas, G. Pierschel, F. Raupach, S. Schael, A. Schultz von Dratzig, G. Schwering, D. Sprenger, M. Thomas, M. Weber, B. Wittmer, M. Wlochal

RWTH Aachen University, III. Physikalisches Institut A, Aachen, Germany

O. Actis, G. Altenhöfer, W. Bender, P. Biallass, M. Erdmann, G. Fetchenhauer¹, J. Frangenheim, T. Hebbeker, G. Hilgers, A. Hinzmann, K. Hoepfner, C. Hof, M. Kirsch, T. Klimkovich, P. Kreuzer¹, D. Lanske[†], M. Merschmeyer, A. Meyer, B. Philipps, H. Pieta, H. Reithler, S.A. Schmitz, L. Sonnenschein, M. Sowa, J. Steggemann, H. Szczesny, D. Teyssier, C. Zeidler

RWTH Aachen University, III. Physikalisches Institut B, Aachen, Germany

M. Bontenackels, M. Davids, M. Duda, G. Flügge, H. Geenen, M. Giffels, W. Haj Ahmad, T. Hermanns, D. Heydhausen, S. Kalinin, T. Kress, A. Linn, A. Nowack, L. Perchalla, M. Poettgens, O. Pooth, P. Sauerland, A. Stahl, D. Tornier, M.H. Zoeller

Deutsches Elektronen-Synchrotron, Hamburg, Germany

M. Aldaya Martin, U. Behrens, K. Borras, A. Campbell, E. Castro, D. Dammann, G. Eckerlin, A. Flossdorf, G. Flucke, A. Geiser, D. Hatton, J. Hauk, H. Jung, M. Kasemann, I. Katkov, C. Kleinwort, H. Kluge, A. Knutsson, E. Kuznetsova, W. Lange, W. Lohmann, R. Mankel¹, M. Marienfeld, A.B. Meyer, S. Miglioranzi, J. Mnich, M. Ohlerich, J. Olzem, A. Parenti, C. Rosemann, R. Schmidt, T. Schoerner-Sadenius, D. Volyansky, C. Wissing, W.D. Zeuner¹

University of Hamburg, Hamburg, Germany

C. Autermann, F. Bechtel, J. Draeger, D. Eckstein, U. Gebbert, K. Kaschube, G. Kaussen, R. Klanner, B. Mura, S. Naumann-Emme, F. Nowak, U. Pein, C. Sander, P. Schlexer, T. Schum, H. Stadie, G. Steinbrück, J. Thomsen, R. Wolf

Institut für Experimentelle Kernphysik, Karlsruhe, Germany

J. Bauer, P. Blüm, V. Buege, A. Cakir, T. Chwalek, W. De Boer, A. Dierlamm, G. Dirkes, M. Feindt, U. Felzmann, M. Frey, A. Furgeri, J. Gruschke, C. Hackstein, F. Hartmann¹, S. Heier, M. Heinrich, H. Held, D. Hirschbuehl, K.H. Hoffmann, S. Honc, C. Jung, T. Kuhr, T. Liamsuwan, D. Martschei, S. Mueller, Th. Müller, M.B. Neuland, M. Niegel, O. Oberst, A. Oehler, J. Ott, T. Peiffer, D. Piparo, G. Quast, K. Rabbertz, F. Ratnikov, N. Ratnikova, M. Renz, C. Saout¹, G. Sartiso, A. Scheurer, P. Schieferdecker, F.-P. Schilling, G. Schott, H.J. Simonis,

F.M. Stober, P. Sturm, D. Troendle, A. Trunov, W. Wagner, J. Wagner-Kuhr, M. Zeise, V. Zhukov⁶, E.B. Ziebarth

Institute of Nuclear Physics "Demokritos", Aghia Paraskevi, Greece

G. Daskalakis, T. Geralis, K. Karafasoulis, A. Kyriakis, D. Loukas, A. Markou, C. Markou, C. Mavrommatis, E. Petrakou, A. Zachariadou

University of Athens, Athens, Greece

L. Gouskos, P. Katsas, A. Panagiotou¹

University of Ioánnina, Ioánnina, Greece

I. Evangelou, P. Kokkas, N. Manthos, I. Papadopoulos, V. Patras, F.A. Triantis

KFKI Research Institute for Particle and Nuclear Physics, Budapest, Hungary

G. Bencze¹, L. Boldizsar, G. Debreczeni, C. Hajdu¹, S. Hernath, P. Hidas, D. Horvath⁷, K. Krajczar, A. Laszlo, G. Patay, F. Sikler, N. Toth, G. Vesztergombi

Institute of Nuclear Research ATOMKI, Debrecen, Hungary

N. Beni, G. Christian, J. Imrek, J. Molnar, D. Novak, J. Palinkas, G. Szekely, Z. Szillasi¹, K. Tokesi, V. Veszpremi

University of Debrecen, Debrecen, Hungary

A. Kapusi, G. Marian, P. Raics, Z. Szabo, Z.L. Trocsanyi, B. Ujvari, G. Zilizi

Panjab University, Chandigarh, India

S. Bansal, H.S. Bawa, S.B. Beri, V. Bhatnagar, M. Jindal, M. Kaur, R. Kaur, J.M. Kohli, M.Z. Mehta, N. Nishu, L.K. Saini, A. Sharma, A. Singh, J.B. Singh, S.P. Singh

University of Delhi, Delhi, India

S. Ahuja, S. Arora, S. Bhattacharya⁸, S. Chauhan, B.C. Choudhary, P. Gupta, S. Jain, S. Jain, M. Jha, A. Kumar, K. Ranjan, R.K. Shivpuri, A.K. Srivastava

Bhabha Atomic Research Centre, Mumbai, India

R.K. Choudhury, D. Dutta, S. Kailas, S.K. Kataria, A.K. Mohanty, L.M. Pant, P. Shukla, A. Topkar

Tata Institute of Fundamental Research - EHEP, Mumbai, India

T. Aziz, M. Guchait⁹, A. Gurtu, M. Maity¹⁰, D. Majumder, G. Majumder, K. Mazumdar, A. Nayak, A. Saha, K. Sudhakar

Tata Institute of Fundamental Research - HECR, Mumbai, India

S. Banerjee, S. Dugad, N.K. Mondal

Institute for Studies in Theoretical Physics & Mathematics (IPM), Tehran, Iran

H. Arfaei, H. Bakhshiansohi, A. Fahim, A. Jafari, M. Mohammadi Najafabadi, A. Moshaii, S. Paktinat Mehdiabadi, S. Rouhani, B. Safarzadeh, M. Zeinali

University College Dublin, Dublin, Ireland

M. Felcini

INFN Sezione di Bari ^a, Università di Bari ^b, Politecnico di Bari ^c, Bari, Italy

M. Abbrescia^{a,b}, L. Barbone^a, F. Chiumarulo^a, A. Clemente^a, A. Colaleo^a, D. Creanza^{a,c}, G. Cuscela^a, N. De Filippis^a, M. De Palma^{a,b}, G. De Robertis^a, G. Donvito^a, F. Fedele^a, L. Fiore^a, M. Franco^a, G. Iaselli^{a,c}, N. Lacalamita^a, F. Loddo^a, L. Lusito^{a,b}, G. Maggi^{a,c}, M. Maggi^a, N. Manna^{a,b}, B. Marangelli^{a,b}, S. My^{a,c}, S. Natali^{a,b}, S. Nuzzo^{a,b}, G. Papagni^a, S. Piccolomo^a, G.A. Pierro^a, C. Pinto^a, A. Pompili^{a,b}, G. Pugliese^{a,c}, R. Rajan^a, A. Ranieri^a, F. Romano^{a,c},

G. Roselli^{a,b}, G. Selvaggi^{a,b}, Y. Shinde^a, L. Silvestris^a, S. Tupputi^{a,b}, G. Zito^a

INFN Sezione di Bologna^a, Università di Bologna^b, Bologna, Italy

G. Abbiendi^a, W. Bacchi^{a,b}, A.C. Benvenuti^a, M. Boldini^a, D. Bonacorsi^a, S. Braibant-Giacomelli^{a,b}, V.D. Cafaro^a, S.S. Caiazza^a, P. Capiluppi^{a,b}, A. Castro^{a,b}, F.R. Cavallo^a, G. Codispoti^{a,b}, M. Cuffiani^{a,b}, I. D'Antone^a, G.M. Dallavalle^{a,1}, F. Fabbri^a, A. Fanfani^{a,b}, D. Fasanella^a, P. Giacomelli^a, V. Giordano^a, M. Giunta^{a,1}, C. Grandi^a, M. Guerzoni^a, S. Marcellini^a, G. Masetti^{a,b}, A. Montanari^a, F.L. Navarra^{a,b}, F. Odorici^a, G. Pellegrini^a, A. Perrotta^a, A.M. Rossi^{a,b}, T. Rovelli^{a,b}, G. Siroli^{a,b}, G. Torromeo^a, R. Travaglini^{a,b}

INFN Sezione di Catania^a, Università di Catania^b, Catania, Italy

S. Albergo^{a,b}, S. Costa^{a,b}, R. Potenza^{a,b}, A. Tricomi^{a,b}, C. Tuve^a

INFN Sezione di Firenze^a, Università di Firenze^b, Firenze, Italy

G. Barbagli^a, G. Broccolo^{a,b}, V. Ciulli^{a,b}, C. Civinini^a, R. D'Alessandro^{a,b}, E. Focardi^{a,b}, S. Frosali^{a,b}, E. Gallo^a, C. Genta^{a,b}, G. Landi^{a,b}, P. Lenzi^{a,b,1}, M. Meschini^a, S. Paoletti^a, G. Sguazzoni^a, A. Tropiano^a

INFN Laboratori Nazionali di Frascati, Frascati, Italy

L. Benussi, M. Bertani, S. Bianco, S. Colafranceschi¹¹, D. Colonna¹¹, F. Fabbri, M. Giardoni, L. Passamonti, D. Piccolo, D. Pierluigi, B. Ponzio, A. Russo

INFN Sezione di Genova, Genova, Italy

P. Fabbriatore, R. Musenich

INFN Sezione di Milano-Bicocca^a, Università di Milano-Bicocca^b, Milano, Italy

A. Benaglia^a, M. Calloni^a, G.B. Cerati^{a,b,1}, P. D'Angelo^a, F. De Guio^a, F.M. Farina^a, A. Ghezzi^a, P. Govoni^{a,b}, M. Malberti^{a,b,1}, S. Malvezzi^a, A. Martelli^a, D. Menasce^a, V. Miccio^{a,b}, L. Moroni^a, P. Negri^{a,b}, M. Paganoni^{a,b}, D. Pedrini^a, A. Pullia^{a,b}, S. Ragazzi^{a,b}, N. Redaelli^a, S. Sala^a, R. Salerno^{a,b}, T. Tabarelli de Fatis^{a,b}, V. Tancini^{a,b}, S. Taroni^{a,b}

INFN Sezione di Napoli^a, Università di Napoli "Federico II"^b, Napoli, Italy

S. Buontempo^a, N. Cavallo^a, A. Cimmino^{a,b,1}, M. De Gruttola^{a,b,1}, F. Fabozzi^{a,12}, A.O.M. Iorio^a, L. Lista^a, D. Lomidze^a, P. Noli^{a,b}, P. Paolucci^a, C. Sciacca^{a,b}

INFN Sezione di Padova^a, Università di Padova^b, Padova, Italy

P. Azzi^{a,1}, N. Bacchetta^a, L. Barcellan^a, P. Bellan^{a,b,1}, M. Bellato^a, M. Benettoni^a, M. Biasotto^{a,13}, D. Bisello^{a,b}, E. Borsato^{a,b}, A. Branca^a, R. Carlin^{a,b}, L. Castellani^a, P. Checchia^a, E. Conti^a, F. Dal Corso^a, M. De Mattia^{a,b}, T. Dorigo^a, U. Dosselli^a, F. Fanzago^a, F. Gasparini^{a,b}, U. Gasparini^{a,b}, P. Giubileo^{a,b}, F. Gonella^a, A. Gresele^{a,14}, M. Gulmini^{a,13}, A. Kaminskiy^{a,b}, S. Lacaprara^{a,13}, I. Lazzizzera^{a,14}, M. Margoni^{a,b}, G. Maron^{a,13}, S. Mattiazzo^{a,b}, M. Mazzucato^a, M. Meneghelli^a, A.T. Meneguzzo^{a,b}, M. Michelotto^a, F. Montecassiano^a, M. Nespolo^a, M. Passaseo^a, M. Pegoraro^a, L. Perrozzi^a, N. Pozzobon^{a,b}, P. Ronchese^{a,b}, F. Simonetto^{a,b}, N. Toniolo^a, E. Torassa^a, M. Tosi^{a,b}, A. Triossi^a, S. Vanini^{a,b}, S. Ventura^a, P. Zotto^{a,b}, G. Zumerle^{a,b}

INFN Sezione di Pavia^a, Università di Pavia^b, Pavia, Italy

P. Baesso^{a,b}, U. Berzano^a, S. Bricola^a, M.M. Necchi^{a,b}, D. Pagano^{a,b}, S.P. Ratti^{a,b}, C. Riccardi^{a,b}, P. Torre^{a,b}, A. Vicini^a, P. Vitulo^{a,b}, C. Viviani^{a,b}

INFN Sezione di Perugia^a, Università di Perugia^b, Perugia, Italy

D. Aisa^a, S. Aisa^a, E. Babucci^a, M. Biasini^{a,b}, G.M. Bilei^a, B. Caponeri^{a,b}, B. Checcucci^a, N. Dinu^a, L. Fanò^a, L. Farnesini^a, P. Lariccia^{a,b}, A. Lucaroni^{a,b}, G. Mantovani^{a,b}, A. Nappi^{a,b}, A. Piluso^a, V. Postolache^a, A. Santocchia^{a,b}, L. Servoli^a, D. Tonoiu^a, A. Vedae^a, R. Volpe^{a,b}

INFN Sezione di Pisa ^a, Universita di Pisa ^b, Scuola Normale Superiore di Pisa ^c, Pisa, Italy
 P. Azzurri^{a,c}, G. Bagliesi^a, J. Bernardini^{a,b}, L. Berretta^a, T. Boccali^a, A. Bocci^{a,c}, L. Borrello^{a,c},
 F. Bosi^a, F. Calzolari^a, R. Castaldi^a, R. Dell’Orso^a, F. Fiori^{a,b}, L. Foà^{a,c}, S. Gennai^{a,c}, A. Giassi^a,
 A. Kraan^a, F. Ligabue^{a,c}, T. Lomtadze^a, F. Mariani^a, L. Martini^a, M. Massa^a, A. Messineo^{a,b},
 A. Moggi^a, F. Palla^a, F. Palmonari^a, G. Petraghani^a, G. Petrucciani^{a,c}, F. Raffaelli^a, S. Sarkar^a,
 G. Segneri^a, A.T. Serban^a, P. Spagnolo^{a,1}, R. Tenchini^{a,1}, S. Tolaini^a, G. Tonelli^{a,b,1}, A. Venturi^a,
 P.G. Verdini^a

INFN Sezione di Roma ^a, Universita di Roma “La Sapienza” ^b, Roma, Italy
 S. Baccaro^{a,15}, L. Barone^{a,b}, A. Bartoloni^a, F. Cavallari^{a,1}, I. Dafinei^a, D. Del Re^{a,b}, E. Di
 Marco^{a,b}, M. Diemoz^a, D. Franci^{a,b}, E. Longo^{a,b}, G. Organtini^{a,b}, A. Palma^{a,b}, F. Pandolfi^{a,b},
 R. Paramatti^{a,1}, F. Pellegrino^a, S. Rahatlou^{a,b}, C. Rovelli^a

**INFN Sezione di Torino ^a, Università di Torino ^b, Università del Piemonte Orientale (No-
 vara) ^c, Torino, Italy**
 G. Alampi^a, N. Amapane^{a,b}, R. Arcidiacono^{a,b}, S. Argiro^{a,b}, M. Arneodo^{a,c}, C. Biino^a,
 M.A. Borgia^{a,b}, C. Botta^{a,b}, N. Cartiglia^a, R. Castello^{a,b}, G. Cerminara^{a,b}, M. Costa^{a,b},
 D. Dattola^a, G. Dellacasa^a, N. Demaria^a, G. Dughera^a, F. Dumitrache^a, A. Graziano^{a,b},
 C. Mariotti^a, M. Marone^{a,b}, S. Maselli^a, E. Migliore^{a,b}, G. Mila^{a,b}, V. Monaco^{a,b}, M. Musich^{a,b},
 M. Nervo^{a,b}, M.M. Obertino^{a,c}, S. Oggero^{a,b}, R. Panero^a, N. Pastrone^a, M. Pelliccioni^{a,b},
 A. Romero^{a,b}, M. Ruspa^{a,c}, R. Sacchi^{a,b}, A. Solano^{a,b}, A. Staiano^a, P.P. Trapani^{a,b,1}, D. Trocino^{a,b},
 A. Vilela Pereira^{a,b}, L. Visca^{a,b}, A. Zampieri^a

INFN Sezione di Trieste ^a, Universita di Trieste ^b, Trieste, Italy
 F. Ambroglini^{a,b}, S. Belforte^a, F. Cossutti^a, G. Della Ricca^{a,b}, B. Gobbo^a, A. Penzo^a

Kyungpook National University, Daegu, Korea
 S. Chang, J. Chung, D.H. Kim, G.N. Kim, D.J. Kong, H. Park, D.C. Son

Wonkwang University, Iksan, Korea
 S.Y. Bahk

Chonnam National University, Kwangju, Korea
 S. Song

Konkuk University, Seoul, Korea
 S.Y. Jung

Korea University, Seoul, Korea
 B. Hong, H. Kim, J.H. Kim, K.S. Lee, D.H. Moon, S.K. Park, H.B. Rhee, K.S. Sim

Seoul National University, Seoul, Korea
 J. Kim

University of Seoul, Seoul, Korea
 M. Choi, G. Hahn, I.C. Park

Sungkyunkwan University, Suwon, Korea
 S. Choi, Y. Choi, J. Goh, H. Jeong, T.J. Kim, J. Lee, S. Lee

Vilnius University, Vilnius, Lithuania
 M. Janulis, D. Martisiute, P. Petrov, T. Sabonis

Centro de Investigacion y de Estudios Avanzados del IPN, Mexico City, Mexico
 H. Castilla Valdez¹, A. Sánchez Hernández

Universidad Iberoamericana, Mexico City, Mexico

S. Carrillo Moreno

Universidad Autónoma de San Luis Potosí, San Luis Potosí, Mexico

A. Morelos Pineda

University of Auckland, Auckland, New Zealand

P. Allfrey, R.N.C. Gray, D. Krofcheck

University of Canterbury, Christchurch, New Zealand

N. Bernardino Rodrigues, P.H. Butler, T. Signal, J.C. Williams

National Centre for Physics, Quaid-I-Azam University, Islamabad, Pakistan

M. Ahmad, I. Ahmed, W. Ahmed, M.I. Asghar, M.I.M. Awan, H.R. Hoorani, I. Hussain, W.A. Khan, T. Khurshid, S. Muhammad, S. Qazi, H. Shahzad

Institute of Experimental Physics, Warsaw, PolandM. Cwiok, R. Dabrowski, W. Dominik, K. Doroba, M. Konecki, J. Krolikowski, K. Pozniak¹⁶, R. Romaniuk, W. Zabolotny¹⁶, P. Zych**Soltan Institute for Nuclear Studies, Warsaw, Poland**

T. Frueboes, R. Gokieli, L. Gosciolo, M. Górski, M. Kazana, K. Nawrocki, M. Szleper, G. Wrochna, P. Zalewski

Laboratório de Instrumentação e Física Experimental de Partículas, Lisboa, Portugal

N. Almeida, L. Antunes Pedro, P. Bargassa, A. David, P. Faccioli, P.G. Ferreira Parracho, M. Freitas Ferreira, M. Gallinaro, M. Guerra Jordao, P. Martins, G. Mini, P. Musella, J. Pela, L. Raposo, P.Q. Ribeiro, S. Sampaio, J. Seixas, J. Silva, P. Silva, D. Soares, M. Sousa, J. Varela, H.K. Wöhri

Joint Institute for Nuclear Research, Dubna, Russia

I. Altsybeev, I. Belotelov, P. Bunin, Y. Ershov, I. Filozova, M. Finger, M. Finger Jr., A. Golunov, I. Golutvin, N. Gorbounov, V. Kalagin, A. Kamenev, V. Karjavin, V. Konoplyanikov, V. Korenkov, G. Kozlov, A. Kurenkov, A. Lanev, A. Makankin, V.V. Mitsyn, P. Moisezenz, E. Nikonov, D. Oleynik, V. Palichik, V. Perelygin, A. Petrosyan, R. Semenov, S. Shmatov, V. Smirnov, D. Smolin, E. Tikhonenko, S. Vasil'ev, A. Vishnevskiy, A. Volodko, A. Zarubin, V. Zhiltsov

Petersburg Nuclear Physics Institute, Gatchina (St Petersburg), Russia

N. Bondar, L. Chtchipounov, A. Denisov, Y. Gavrikov, G. Gavrilo, V. Golovtsov, Y. Ivanov, V. Kim, V. Kozlov, P. Levchenko, G. Obrant, E. Orishchin, A. Petrunin, Y. Shcheglov, A. Shchetkovskiy, V. Sknar, I. Smirnov, V. Sulimov, V. Tarakanov, L. Uvarov, S. Vavilov, G. Velichko, S. Volkov, A. Vorobyev

Institute for Nuclear Research, Moscow, Russia

Yu. Andreev, A. Anisimov, P. Antipov, A. Dermenev, S. Gninenko, N. Golubev, M. Kirsanov, N. Krasnikov, V. Matveev, A. Pashenkov, V.E. Postoev, A. Solovey, A. Solovey, A. Toropin, S. Troitsky

Institute for Theoretical and Experimental Physics, Moscow, RussiaA. Baud, V. Epshteyn, V. Gavrilov, N. Ilina, V. Kaftanov[†], V. Kolosov, M. Kossov¹, A. Krokhotin, S. Kuleshov, A. Oulianov, G. Safronov, S. Semenov, I. Shreyber, V. Stolin, E. Vlasov, A. Zhokin**Moscow State University, Moscow, Russia**E. Boos, M. Dubinin¹⁷, L. Dudko, A. Ershov, A. Gribushin, V. Klyukhin, O. Kodolova, I. Lokhtin, S. Petrushanko, L. Sarycheva, V. Savrin, A. Snigirev, I. Vardanyan

P.N. Lebedev Physical Institute, Moscow, Russia

I. Dremin, M. Kirakosyan, N. Konvalova, S.V. Rusakov, A. Vinogradov

State Research Center of Russian Federation, Institute for High Energy Physics, Protvino, Russia

S. Akimenko, A. Artamonov, I. Azhgirey, S. Bitioukov, V. Burtovoy, V. Grishin¹, V. Kachanov, D. Konstantinov, V. Krychkine, A. Levine, I. Lobov, V. Lukanin, Y. Mel'nik, V. Petrov, R. Ryutin, S. Slabospitsky, A. Sobol, A. Sytine, L. Tourtchanovitch, S. Troshin, N. Tyurin, A. Uzunian, A. Volkov

Vinca Institute of Nuclear Sciences, Belgrade, Serbia

P. Adzic, M. Djordjevic, D. Jovanovic¹⁸, D. Krpic¹⁸, D. Maletic, J. Puzovic¹⁸, N. Smiljkovic

Centro de Investigaciones Energéticas Medioambientales y Tecnológicas (CIEMAT), Madrid, Spain

M. Aguilar-Benitez, J. Alberdi, J. Alcaraz Maestre, P. Arce, J.M. Barcala, C. Battilana, C. Burgos Lazaro, J. Caballero Bejar, E. Calvo, M. Cardenas Montes, M. Cepeda, M. Cerrada, M. Chamizo Llatas, F. Clemente, N. Colino, M. Daniel, B. De La Cruz, A. Delgado Peris, C. Diez Pardos, C. Fernandez Bedoya, J.P. Fernández Ramos, A. Ferrando, J. Flix, M.C. Fouz, P. Garcia-Abia, A.C. Garcia-Bonilla, O. Gonzalez Lopez, S. Goy Lopez, J.M. Hernandez, M.I. Josa, J. Marin, G. Merino, J. Molina, A. Molinero, J.J. Navarrete, J.C. Oller, J. Puerta Pelayo, L. Romero, J. Santaolalla, C. Villanueva Munoz, C. Willmott, C. Yuste

Universidad Autónoma de Madrid, Madrid, Spain

C. Albajar, M. Blanco Otano, J.F. de Trocóniz, A. Garcia Raboso, J.O. Lopez Berengueres

Universidad de Oviedo, Oviedo, Spain

J. Cuevas, J. Fernandez Menendez, I. Gonzalez Caballero, L. Lloret Iglesias, H. Naves Sordo, J.M. Vizan Garcia

Instituto de Física de Cantabria (IFCA), CSIC-Universidad de Cantabria, Santander, Spain

I.J. Cabrillo, A. Calderon, S.H. Chuang, I. Diaz Merino, C. Diez Gonzalez, J. Duarte Campderros, M. Fernandez, G. Gomez, J. Gonzalez Sanchez, R. Gonzalez Suarez, C. Jorda, P. Lobelle Pardo, A. Lopez Virto, J. Marco, R. Marco, C. Martinez Rivero, P. Martinez Ruiz del Arbol, F. Matorras, T. Rodrigo, A. Ruiz Jimeno, L. Scodellaro, M. Sobron Sanudo, I. Vila, R. Vilar Cortabitarte

CERN, European Organization for Nuclear Research, Geneva, Switzerland

D. Abbaneo, E. Albert, M. Alidra, S. Ashby, E. Auffray, J. Baechler, P. Baillon, A.H. Ball, S.L. Bally, D. Barney, F. Beaudette¹⁹, R. Bellan, D. Benedetti, G. Benelli, C. Bernet, P. Bloch, S. Bolognesi, M. Bona, J. Bos, N. Bourgeois, T. Bourrel, H. Breuker, K. Bunkowski, D. Campi, T. Camporesi, E. Cano, A. Cattai, J.P. Chatelain, M. Chauvey, T. Christiansen, J.A. Coarasa Perez, A. Conde Garcia, R. Covarelli, B. Curé, A. De Roeck, V. Delachenal, D. Deyrail, S. Di Vincenzo²⁰, S. Dos Santos, T. Dupont, L.M. Edera, A. Elliott-Peisert, M. Eppard, M. Favre, N. Frank, W. Funk, A. Gaddi, M. Gastal, M. Gateau, H. Gerwig, D. Gigi, K. Gill, D. Giordano, J.P. Girod, F. Glege, R. Gomez-Reino Garrido, R. Goudard, S. Gowdy, R. Guida, L. Guiducci, J. Gutleber, M. Hansen, C. Hartl, J. Harvey, B. Hegner, H.F. Hoffmann, A. Holzner, A. Honma, M. Huhtinen, V. Innocente, P. Janot, G. Le Godec, P. Lecoq, C. Leonidopoulos, R. Loos, C. Lourenço, A. Lyonnet, A. Macpherson, N. Magini, J.D. Maillefaud, G. Maire, T. Mäki, L. Malgeri, M. Mannelli, L. Masetti, F. Meijers, P. Meridiani, S. Mersi, E. Meschi, A. Meynet Cordonnier, R. Moser, M. Mulders, J. Mulon, M. Noy, A. Oh, G. Olesen, A. Onnela, T. Orimoto, L. Orsini, E. Perez, G. Perinic, J.F. Pernot, P. Petagna, P. Petiot, A. Petrilli, A. Pfeiffer, M. Pierini, M. Pimiä, R. Pintus, B. Pirollet, H. Postema, A. Racz, S. Ravat, S.B. Rew, J. Rodrigues Antunes,

G. Rolandi²¹, M. Rovere, V. Ryjov, H. Sakulin, D. Samyn, H. Sauce, C. Schäfer, W.D. Schlatter, M. Schröder, C. Schwick, A. Sciaba, I. Segoni, A. Sharma, N. Siegrist, P. Siegrist, N. Sinanis, T. Sobrier, P. Sphicas²², D. Spiga, M. Spiropulu¹⁷, F. Stöckli, P. Traczyk, P. Tropea, J. Troska, A. Tsirou, L. Veillet, G.I. Veres, M. Voutilainen, P. Wertelaers, M. Zanetti

Paul Scherrer Institut, Villigen, Switzerland

W. Bertl, K. Deiters, W. Erdmann, K. Gabathuler, R. Horisberger, Q. Ingram, H.C. Kaestli, S. König, D. Kotlinski, U. Langenegger, F. Meier, D. Renker, T. Rohe, J. Sibille²³, A. Starodumov²⁴

Institute for Particle Physics, ETH Zurich, Zurich, Switzerland

B. Betev, L. Caminada²⁵, Z. Chen, S. Cittolin, D.R. Da Silva Di Calafiori, S. Dambach²⁵, G. Dissertori, M. Dittmar, C. Eggel²⁵, J. Eugster, G. Faber, K. Freudenreich, C. Grab, A. Hervé, W. Hintz, P. Lecomte, P.D. Luckey, W. Lustermann, C. Marchica²⁵, P. Milenovic²⁶, F. Moortgat, A. Nardulli, F. Nessi-Tedaldi, L. Pape, F. Pauss, T. Punz, A. Rizzi, F.J. Ronga, L. Sala, A.K. Sanchez, M.-C. Sawley, V. Sordini, B. Stieger, L. Tauscher[†], A. Thea, K. Theofilatos, D. Treille, P. Trüb²⁵, M. Weber, L. Wehrli, J. Weng, S. Zelepoukine²⁷

Universität Zürich, Zurich, Switzerland

C. AMSLER, V. Chiochia, S. De Visscher, C. Regenfus, P. Robmann, T. Rommerskirchen, A. Schmidt, D. Tsirigkas, L. Wilke

National Central University, Chung-Li, Taiwan

Y.H. Chang, E.A. Chen, W.T. Chen, A. Go, C.M. Kuo, S.W. Li, W. Lin

National Taiwan University (NTU), Taipei, Taiwan

P. Bartalini, P. Chang, Y. Chao, K.F. Chen, W.-S. Hou, Y. Hsiung, Y.J. Lei, S.W. Lin, R.-S. Lu, J. Schümann, J.G. Shiu, Y.M. Tzeng, K. Ueno, Y. Velikzhanin, C.C. Wang, M. Wang

Cukurova University, Adana, Turkey

A. Adiguzel, A. Ayhan, A. Azman Gokce, M.N. Bakirci, S. Cerci, I. Dumanoglu, E. Eskut, S. Girgis, E. Gurpinar, I. Hos, T. Karaman, T. Karaman, A. Kayis Topaksu, P. Kurt, G. Önengüt, G. Önengüt Gökbulut, K. Ozdemir, S. Ozturk, A. Polatöz, K. Sogut²⁸, B. Tali, H. Topakli, D. Uzun, L.N. Vergili, M. Vergili

Middle East Technical University, Physics Department, Ankara, Turkey

I.V. Akin, T. Aliev, S. Bilmis, M. Deniz, H. Gamsizkan, A.M. Guler, K. Öcalan, M. Serin, R. Sever, U.E. Surat, M. Zeyrek

Bogaziçi University, Department of Physics, Istanbul, Turkey

M. Deliomeroglu, D. Demir²⁹, E. Gülmez, A. Halu, B. Isildak, M. Kaya³⁰, O. Kaya³⁰, S. Ozkorucuklu³¹, N. Sonmez³²

National Scientific Center, Kharkov Institute of Physics and Technology, Kharkov, Ukraine

L. Levchuk, S. Lukyanenko, D. Soroka, S. Zub

University of Bristol, Bristol, United Kingdom

F. Bostock, J.J. Brooke, T.L. Cheng, D. Cussans, R. Frazier, J. Goldstein, N. Grant, M. Hansen, G.P. Heath, H.F. Heath, C. Hill, B. Huckvale, J. Jackson, C.K. Mackay, S. Metson, D.M. Newbold³³, K. Nirunpong, V.J. Smith, J. Velthuis, R. Walton

Rutherford Appleton Laboratory, Didcot, United Kingdom

K.W. Bell, C. Brew, R.M. Brown, B. Camanzi, D.J.A. Cockerill, J.A. Coughlan, N.I. Geddes, K. Harder, S. Harper, B.W. Kennedy, P. Murray, C.H. Shepherd-Themistocleous, I.R. Tomalin, J.H. Williams[†], W.J. Womersley, S.D. Worm

Imperial College, University of London, London, United Kingdom

R. Bainbridge, G. Ball, J. Ballin, R. Beuselinck, O. Buchmuller, D. Colling, N. Cripps, G. Davies, M. Della Negra, C. Foudas, J. Fulcher, D. Futyan, G. Hall, J. Hays, G. Iles, G. Karapostoli, B.C. MacEvoy, A.-M. Magnan, J. Marrouche, J. Nash, A. Nikitenko²⁴, A. Papageorgiou, M. Pesaresi, K. Petridis, M. Pioppi³⁴, D.M. Raymond, N. Rompotis, A. Rose, M.J. Ryan, C. Seez, P. Sharp, G. Sidiropoulos¹, M. Stettler, M. Stoye, M. Takahashi, A. Tapper, C. Timlin, S. Tourneur, M. Vazquez Acosta, T. Virdee¹, S. Wakefield, D. Wardrope, T. Whyntie, M. Wingham

Brunel University, Uxbridge, United Kingdom

J.E. Cole, I. Goitom, P.R. Hobson, A. Khan, P. Kyberd, D. Leslie, C. Munro, I.D. Reid, C. Siमितros, R. Taylor, L. Teodorescu, I. Yaselli

Boston University, Boston, USA

T. Bose, M. Carleton, E. Hazen, A.H. Heering, A. Heister, J. St. John, P. Lawson, D. Lazic, D. Osborne, J. Rohlf, L. Sulak, S. Wu

Brown University, Providence, USA

J. Andrea, A. Avetisyan, S. Bhattacharya, J.P. Chou, D. Cutts, S. Esen, G. Kukartsev, G. Landsberg, M. Narain, D. Nguyen, T. Speer, K.V. Tsang

University of California, Davis, Davis, USA

R. Breedon, M. Calderon De La Barca Sanchez, M. Case, D. Cebra, M. Chertok, J. Conway, P.T. Cox, J. Dolen, R. Erbacher, E. Friis, W. Ko, A. Kopecky, R. Lander, A. Lister, H. Liu, S. Maruyama, T. Miceli, M. Nikolic, D. Pellett, J. Robles, M. Searle, J. Smith, M. Squires, J. Stilley, M. Tripathi, R. Vasquez Sierra, C. Veelken

University of California, Los Angeles, Los Angeles, USA

V. Andreev, K. Arisaka, D. Cline, R. Cousins, S. Erhan¹, J. Hauser, M. Ignatenko, C. Jarvis, J. Mumford, C. Plager, G. Rakness, P. Schlein[†], J. Tucker, V. Valuev, R. Wallny, X. Yang

University of California, Riverside, Riverside, USA

J. Babb, M. Bose, A. Chandra, R. Clare, J.A. Ellison, J.W. Gary, G. Hanson, G.Y. Jeng, S.C. Kao, F. Liu, H. Liu, A. Luthra, H. Nguyen, G. Pasztor³⁵, A. Satpathy, B.C. Shen[†], R. Stringer, J. Sturdy, V. Sytnik, R. Wilken, S. Wimpenny

University of California, San Diego, La Jolla, USA

J.G. Branson, E. Dusinger, D. Evans, F. Golf, R. Kelley, M. Lebourgeois, J. Letts, E. Lipeles, B. Mangano, J. Muelmenstaedt, M. Norman, S. Padhi, A. Petrucci, H. Pi, M. Pieri, R. Ranieri, M. Sani, V. Sharma, S. Simon, F. Würthwein, A. Yagil

University of California, Santa Barbara, Santa Barbara, USA

C. Campagnari, M. D'Alfonso, T. Danielson, J. Garbersson, J. Incandela, C. Justus, P. Kalavase, S.A. Koay, D. Kovalskyi, V. Krutelyov, J. Lamb, S. Lowette, V. Pavlunin, F. Rebassoo, J. Ribnik, J. Richman, R. Rossin, D. Stuart, W. To, J.R. Vlimant, M. Witherell

California Institute of Technology, Pasadena, USA

A. Apresyan, A. Bornheim, J. Bunn, M. Chiorboli, M. Gataullin, D. Kcira, V. Litvine, Y. Ma, H.B. Newman, C. Rogan, V. Timciuc, J. Veverka, R. Wilkinson, Y. Yang, L. Zhang, K. Zhu, R.Y. Zhu

Carnegie Mellon University, Pittsburgh, USA

B. Akgun, R. Carroll, T. Ferguson, D.W. Jang, S.Y. Jun, M. Paulini, J. Russ, N. Terentyev, H. Vogel, I. Vorobiev

University of Colorado at Boulder, Boulder, USA

J.P. Cumalat, M.E. Dinardo, B.R. Drell, W.T. Ford, B. Heyburn, E. Luiggi Lopez, U. Nauenberg, K. Stenson, K. Ulmer, S.R. Wagner, S.L. Zang

Cornell University, Ithaca, USA

L. Agostino, J. Alexander, F. Blekman, D. Cassel, A. Chatterjee, S. Das, L.K. Gibbons, B. Heltsley, W. Hopkins, A. Khukhunaishvili, B. Kreis, V. Kuznetsov, J.R. Patterson, D. Puigh, A. Ryd, X. Shi, S. Stroiney, W. Sun, W.D. Teo, J. Thom, J. Vaughan, Y. Weng, P. Wittich

Fairfield University, Fairfield, USA

C.P. Beetz, G. Cirino, C. Sanzeni, D. Winn

Fermi National Accelerator Laboratory, Batavia, USA

S. Abdullin, M.A. Afaq¹, M. Albrow, B. Ananthan, G. Apollinari, M. Atac, W. Badgett, L. Bagby, J.A. Bakken, B. Baldin, S. Banerjee, K. Banicz, L.A.T. Bauerdick, A. Beretvas, J. Berryhill, P.C. Bhat, K. Biery, M. Binkley, I. Bloch, F. Borcherding, A.M. Brett, K. Burkett, J.N. Butler, V. Chetluru, H.W.K. Cheung, F. Chlebana, I. Churin, S. Cihangir, M. Crawford, W. Dagenhart, M. Demarteau, G. Derylo, D. Dykstra, D.P. Eartly, J.E. Elias, V.D. Elvira, D. Evans, L. Feng, M. Fischler, I. Fisk, S. Foulkes, J. Freeman, P. Gartung, E. Gottschalk, T. Grassi, D. Green, Y. Guo, O. Gutsche, A. Hahn, J. Hanlon, R.M. Harris, B. Holzman, J. Howell, D. Hufnagel, E. James, H. Jensen, M. Johnson, C.D. Jones, U. Joshi, E. Juska, J. Kaiser, B. Klima, S. Kossiakov, K. Kousouris, S. Kwan, C.M. Lei, P. Limon, J.A. Lopez Perez, S. Los, L. Lueking, G. Lukhanin, S. Lusin¹, J. Lykken, K. Maeshima, J.M. Marraffino, D. Mason, P. McBride, T. Miao, K. Mishra, S. Moccia, R. Mommsen, S. Mrenna, A.S. Muhammad, C. Newman-Holmes, C. Noeding, V. O'Dell, O. Prokofyev, R. Rivera, C.H. Rivetta, A. Ronzhin, P. Rossman, S. Ryu, V. Sekhri, E. Sexton-Kennedy, I. Sfiligoi, S. Sharma, T.M. Shaw, D. Shpakov, E. Skup, R.P. Smith[†], A. Soha, W.J. Spalding, L. Spiegel, I. Suzuki, P. Tan, W. Tanenbaum, S. Tkaczyk¹, R. Trentadue¹, L. Up-
legger, E.W. Vaandering, R. Vidal, J. Whitmore, E. Wicklund, W. Wu, J. Yarba, F. Yumiceva, J.C. Yun

University of Florida, Gainesville, USA

D. Acosta, P. Avery, V. Barashko, D. Bourilkov, M. Chen, G.P. Di Giovanni, D. Dobur, A. Drozdetskiy, R.D. Field, Y. Fu, I.K. Furic, J. Gartner, D. Holmes, B. Kim, S. Klimentko, J. Konigsberg, A. Korytov, K. Kotov, A. Kropivnitskaya, T. Kypreos, A. Madorsky, K. Matchev, G. Mitselmakher, Y. Pakhotin, J. Piedra Gomez, C. Prescott, V. Rapsevicius, R. Remington, M. Schmitt, B. Scurlock, D. Wang, J. Yelton

Florida International University, Miami, USA

C. Ceron, V. Gaultney, L. Kramer, L.M. Lebolo, S. Linn, P. Markowitz, G. Martinez, J.L. Rodriguez

Florida State University, Tallahassee, USA

T. Adams, A. Askew, H. Baer, M. Bertoldi, J. Chen, W.G.D. Dharmaratna, S.V. Gleyzer, J. Haas, S. Hagopian, V. Hagopian, M. Jenkins, K.F. Johnson, E. Prettner, H. Prosper, S. Sekmen

Florida Institute of Technology, Melbourne, USA

M.M. Baarmand, S. Guragain, M. Hohmann, H. Kalakhety, H. Mermerkaya, R. Ralich, I. Vodopyanov

University of Illinois at Chicago (UIC), Chicago, USA

B. Abelev, M.R. Adams, I.M. Anghel, L. Apanasevich, V.E. Bazterra, R.R. Betts, J. Callner, M.A. Castro, R. Cavanaugh, C. Dragoiu, E.J. Garcia-Solis, C.E. Gerber, D.J. Hofman, S. Khalatian, C. Mironov, E. Shabalina, A. Smoron, N. Varelas

The University of Iowa, Iowa City, USA

U. Akgun, E.A. Albayrak, A.S. Ayan, B. Bilki, R. Briggs, K. Cankocak³⁶, K. Chung, W. Clarida, P. Debbins, F. Duru, F.D. Ingram, C.K. Lae, E. McCliment, J.-P. Merlo, A. Mestvirishvili, M.J. Miller, A. Moeller, J. Nachtman, C.R. Newsom, E. Norbeck, J. Olson, Y. Onel, F. Ozok, J. Parsons, I. Schmidt, S. Sen, J. Wetzel, T. Yetkin, K. Yi

Johns Hopkins University, Baltimore, USA

B.A. Barnett, B. Blumenfeld, A. Bonato, C.Y. Chien, D. Fehling, G. Giurciu, A.V. Gritsan, Z.J. Guo, P. Maksimovic, S. Rappoccio, M. Swartz, N.V. Tran, Y. Zhang

The University of Kansas, Lawrence, USA

P. Baringer, A. Bean, O. Grachov, M. Murray, V. Radicci, S. Sanders, J.S. Wood, V. Zhukova

Kansas State University, Manhattan, USA

D. Bandurin, T. Bolton, K. Kaadze, A. Liu, Y. Maravin, D. Onoprienko, I. Svintradze, Z. Wan

Lawrence Livermore National Laboratory, Livermore, USA

J. Gronberg, J. Hollar, D. Lange, D. Wright

University of Maryland, College Park, USA

D. Baden, R. Bard, M. Boutemour, S.C. Eno, D. Ferencek, N.J. Hadley, R.G. Kellogg, M. Kirn, S. Kunori, K. Rossato, P. Rumerio, F. Santanastasio, A. Skuja, J. Temple, M.B. Tonjes, S.C. Tonwar, T. Toole, E. Twedt

Massachusetts Institute of Technology, Cambridge, USA

B. Alver, G. Bauer, J. Bendavid, W. Busza, E. Butz, I.A. Cali, M. Chan, D. D'Enterria, P. Everaerts, G. Gomez Ceballos, K.A. Hahn, P. Harris, S. Jaditz, Y. Kim, M. Klute, Y.-J. Lee, W. Li, C. Loizides, T. Ma, M. Miller, S. Nahn, C. Paus, C. Roland, G. Roland, M. Rudolph, G. Stephans, K. Sumorok, K. Sung, S. Vaurynovich, E.A. Wenger, B. Wyslouch, S. Xie, Y. Yilmaz, A.S. Yoon

University of Minnesota, Minneapolis, USA

D. Bailleux, S.I. Cooper, P. Cushman, B. Dahmes, A. De Benedetti, A. Dolgoplov, P.R. Duderod, R. Egeland, G. Franzoni, J. Haupt, A. Inyakin³⁷, K. Klappoetke, Y. Kubota, J. Mans, N. Mirman, D. Petyt, V. Rekovic, R. Rusack, M. Schroeder, A. Singovsky, J. Zhang

University of Mississippi, University, USA

L.M. Cremaldi, R. Godang, R. Kroeger, L. Perera, R. Rahmat, D.A. Sanders, P. Sonnek, D. Summers

University of Nebraska-Lincoln, Lincoln, USA

K. Bloom, B. Bockelman, S. Bose, J. Butt, D.R. Claes, A. Dominguez, M. Eads, J. Keller, T. Kelly, I. Kravchenko, J. Lazo-Flores, C. Lundstedt, H. Malbouisson, S. Malik, G.R. Snow

State University of New York at Buffalo, Buffalo, USA

U. Baur, I. Iashvili, A. Kharchilava, A. Kumar, K. Smith, M. Strang

Northeastern University, Boston, USA

G. Alverson, E. Barberis, O. Boeriu, G. Eulisse, G. Govi, T. McCauley, Y. Musienko³⁸, S. Muzaffar, I. Osborne, T. Paul, S. Reucroft, J. Swain, L. Taylor, L. Tuura

Northwestern University, Evanston, USA

A. Anastassov, B. Gobbi, A. Kubik, R.A. Ofierzynski, A. Pozdnyakov, M. Schmitt, S. Stoynev, M. Velasco, S. Won

University of Notre Dame, Notre Dame, USA

L. Antonelli, D. Berry, M. Hildreth, C. Jessop, D.J. Karmgard, T. Kolberg, K. Lannon, S. Lynch,

N. Marinelli, D.M. Morse, R. Ruchti, J. Slaunwhite, J. Warchol, M. Wayne

The Ohio State University, Columbus, USA

B. Bylsma, L.S. Durkin, J. Gilmore³⁹, J. Gu, P. Killewald, T.Y. Ling, G. Williams

Princeton University, Princeton, USA

N. Adam, E. Berry, P. Elmer, A. Garmash, D. Gerbaudo, V. Halyo, A. Hunt, J. Jones, E. Laird, D. Marlow, T. Medvedeva, M. Mooney, J. Olsen, P. Piroué, D. Stickland, C. Tully, J.S. Werner, T. Wildish, Z. Xie, A. Zuranski

University of Puerto Rico, Mayaguez, USA

J.G. Acosta, M. Bonnett Del Alamo, X.T. Huang, A. Lopez, H. Mendez, S. Oliveros, J.E. Ramirez Vargas, N. Santacruz, A. Zatzerklyany

Purdue University, West Lafayette, USA

E. Alagoz, E. Antillon, V.E. Barnes, G. Bolla, D. Bortoletto, A. Everett, A.F. Garfinkel, Z. Gecse, L. Gutay, N. Ippolito, M. Jones, O. Koybasi, A.T. Laasanen, N. Leonardo, C. Liu, V. Maroussov, P. Merkel, D.H. Miller, N. Neumeister, A. Sedov, I. Shipsey, H.D. Yoo, Y. Zheng

Purdue University Calumet, Hammond, USA

P. Jindal, N. Parashar

Rice University, Houston, USA

V. Cuplov, K.M. Ecklund, F.J.M. Geurts, J.H. Liu, D. Maronde, M. Matveev, B.P. Padley, R. Redjimi, J. Roberts, L. Sabbatini, A. Tumanov

University of Rochester, Rochester, USA

B. Betchart, A. Bodek, H. Budd, Y.S. Chung, P. de Barbaro, R. Demina, H. Flacher, Y. Gotra, A. Harel, S. Korjenevski, D.C. Miner, D. Orbaker, G. Petrillo, D. Vishnevskiy, M. Zielinski

The Rockefeller University, New York, USA

A. Bhatti, L. Demortier, K. Goulianos, K. Hatakeyama, G. Lungu, C. Mesropian, M. Yan

Rutgers, the State University of New Jersey, Piscataway, USA

O. Atramentov, E. Bartz, Y. Gershtein, E. Halkiadakis, D. Hits, A. Lath, K. Rose, S. Schnetzer, S. Somalwar, R. Stone, S. Thomas, T.L. Watts

University of Tennessee, Knoxville, USA

G. Cerizza, M. Hollingsworth, S. Spanier, Z.C. Yang, A. York

Texas A&M University, College Station, USA

J. Asaadi, A. Aurisano, R. Eusebi, A. Golyash, A. Gurrola, T. Kamon, C.N. Nguyen, J. Pivarski, A. Safonov, S. Sengupta, D. Toback, M. Weinberger

Texas Tech University, Lubbock, USA

N. Akchurin, L. Berntzon, K. Gumus, C. Jeong, H. Kim, S.W. Lee, S. Popescu, Y. Roh, A. Sill, I. Volobouev, E. Washington, R. Wigmans, E. Yazgan

Vanderbilt University, Nashville, USA

D. Engh, C. Florez, W. Johns, S. Pathak, P. Sheldon

University of Virginia, Charlottesville, USA

D. Andelin, M.W. Arenton, M. Balazs, S. Boutle, M. Buehler, S. Conetti, B. Cox, R. Hirosky, A. Ledovskoy, C. Neu, D. Phillips II, M. Ronquest, R. Yohay

Wayne State University, Detroit, USA

S. Gollapinni, K. Gunthoti, R. Harr, P.E. Karchin, M. Mattson, A. Sakharov

University of Wisconsin, Madison, USA

M. Anderson, M. Bachtis, J.N. Bellinger, D. Carlsmith, I. Crotty¹, S. Dasu, S. Dutta, J. Efron, F. Feyzi, K. Flood, L. Gray, K.S. Grogg, M. Grothe, R. Hall-Wilton¹, M. Jaworski, P. Klabbers, J. Klukas, A. Lanaro, C. Lazaridis, J. Leonard, R. Loveless, M. Magrans de Abril, A. Mohapatra, G. Ott, G. Polese, D. Reeder, A. Savin, W.H. Smith, A. Sourkov⁴⁰, J. Swanson, M. Weinberg, D. Wenman, M. Wensveen, A. White

†: Deceased

1: Also at CERN, European Organization for Nuclear Research, Geneva, Switzerland

2: Also at Universidade Federal do ABC, Santo Andre, Brazil

3: Also at Soltan Institute for Nuclear Studies, Warsaw, Poland

4: Also at Université de Haute-Alsace, Mulhouse, France

5: Also at Centre de Calcul de l'Institut National de Physique Nucleaire et de Physique des Particules (IN2P3), Villeurbanne, France

6: Also at Moscow State University, Moscow, Russia

7: Also at Institute of Nuclear Research ATOMKI, Debrecen, Hungary

8: Also at University of California, San Diego, La Jolla, USA

9: Also at Tata Institute of Fundamental Research - HECR, Mumbai, India

10: Also at University of Visva-Bharati, Santiniketan, India

11: Also at Facolta' Ingegneria Universita' di Roma "La Sapienza", Roma, Italy

12: Also at Università della Basilicata, Potenza, Italy

13: Also at Laboratori Nazionali di Legnaro dell' INFN, Legnaro, Italy

14: Also at Università di Trento, Trento, Italy

15: Also at ENEA - Casaccia Research Center, S. Maria di Galeria, Italy

16: Also at Warsaw University of Technology, Institute of Electronic Systems, Warsaw, Poland

17: Also at California Institute of Technology, Pasadena, USA

18: Also at Faculty of Physics of University of Belgrade, Belgrade, Serbia

19: Also at Laboratoire Leprince-Ringuet, Ecole Polytechnique, IN2P3-CNRS, Palaiseau, France

20: Also at Alstom Contracting, Geneve, Switzerland

21: Also at Scuola Normale e Sezione dell' INFN, Pisa, Italy

22: Also at University of Athens, Athens, Greece

23: Also at The University of Kansas, Lawrence, USA

24: Also at Institute for Theoretical and Experimental Physics, Moscow, Russia

25: Also at Paul Scherrer Institut, Villigen, Switzerland

26: Also at Vinca Institute of Nuclear Sciences, Belgrade, Serbia

27: Also at University of Wisconsin, Madison, USA

28: Also at Mersin University, Mersin, Turkey

29: Also at Izmir Institute of Technology, Izmir, Turkey

30: Also at Kafkas University, Kars, Turkey

31: Also at Suleyman Demirel University, Isparta, Turkey

32: Also at Ege University, Izmir, Turkey

33: Also at Rutherford Appleton Laboratory, Didcot, United Kingdom

34: Also at INFN Sezione di Perugia; Universita di Perugia, Perugia, Italy

35: Also at KFKI Research Institute for Particle and Nuclear Physics, Budapest, Hungary

36: Also at Istanbul Technical University, Istanbul, Turkey

37: Also at University of Minnesota, Minneapolis, USA

38: Also at Institute for Nuclear Research, Moscow, Russia

39: Also at Texas A&M University, College Station, USA

40: Also at State Research Center of Russian Federation, Institute for High Energy Physics, Protvino, Russia

